



Field Trip Guide Book - B10

Florence - Italy
August 20-28, 2004

Volume n° 1 - from PR01 to B15

32nd INTERNATIONAL GEOLOGICAL CONGRESS

ACTIVE TECTONICS IN THE MEDITERRANEAN SECTOR OF THE IBERIAN PENINSULA (EAST SPAIN)



Leaders:

*G.P. Silva, P. Alfaro, E. Masana,
J.J. Martínez Díaz, T. Bardají*

*Associate Leaders: A. Estévez, J.L. Goy,
P. Santanach, C. Zazo, K.R. Reicherter*

Pre-Congress

B10

The scientific content of this guide is under the total responsibility of the Authors

Published by:

**APAT – Italian Agency for the Environmental Protection and Technical Services - Via Vitaliano
Brancati, 48 - 00144 Roma - Italy**



Series Editors:

Luca Guerrieri, Irene Rischia and Leonello Serva (APAT, Roma)

English Desk-copy Editors:

Paul Mazza (Università di Firenze), Jessica Ann Thonn (Università di Firenze), Nathalie Marlène Adams (Università di Firenze), Miriam Friedman (Università di Firenze), Kate Eadie (Freelance independent professional)

Field Trip Committee:

Leonello Serva (APAT, Roma), Alessandro Michetti (Università dell'Insubria, Como), Giulio Pavia (Università di Torino), Raffaele Pignone (Servizio Geologico Regione Emilia-Romagna, Bologna) and Riccardo Polino (CNR, Torino)

Acknowledgments:

The 32nd IGC Organizing Committee is grateful to Roberto Pompili and Elisa Brustia (APAT, Roma) for their collaboration in editing.

Graphic project:

Full snc - Firenze

Layout and press:

Lito Terrazzi srl - Firenze

Volume n°1 - da PR01 a B15



**32nd INTERNATIONAL
GEOLOGICAL CONGRESS**

**ACTIVE TECTONICS IN THE
MEDITERRANEAN SECTOR OF THE
IBERIAN PENINSULA (EAST SPAIN)**

LEADERS:

G.P. Silva¹, P. Alfaro², E. Masana³, J.J. Martínez Díaz⁴, T. Bardají⁵

ASSOCIATE LEADERS:

A. Estévez³, J.L. Goy⁶, P. Santanach², C. Zazo⁷, K.R. Reicherter⁸

¹ *Departamento de Geología, Universidad de Salamanca, Avila - Spain*

² *Departament de Geologia Dinàmica i Geofísica, Barcelona - Spain*

³ *Departamento CC. de la Tierra y del Medio Ambiente, Alicante - Spain*

⁴ *Departamento de Geodinámica, Universidad Complutense de Madrid, Madrid - Spain*

⁵ *Departamento de Geología, Universidad de Alcalá de Henares, Madrid - Spain*

⁶ *Departamento de Geología, Universidad de Salamanca, Salamanca - Spain*

⁷ *Departamento de Geología, Museo Nac. CC. Naturales (CSIC), Madrid - Spain*

⁸ *Institut für Geophysik und Geologie (IGG), Leipzig - Germany*

**Florence - Italy
August 20-28, 2004**

Pre-Congress

B10

Front Cover:
*Multibanded fault gouge of the Carboneras Fault zone
at Sopalmo (Almería). Photo T. Bardaji.*

Leaders: G.P. Silva, P. Alfaro, E. Masana, J.J. Martínez Díaz, T. Bardají

Introduction

P.G. Silva

This field trip develops in the context of The Eastern Betics Shear Zone (EBSZ, SE Spain) and the Catalan Coastal Ranges (CCR, NE Spain) along the Mediterranean portion of the Iberian Peninsula. Neotectonics, Structural Geology, Tectonic Geomorphology and Paleoseismology are the main topics, providing an integrated approach to the earthquake geology and seismic hazard of the areas visited. The trip will start in Almería, at the southern

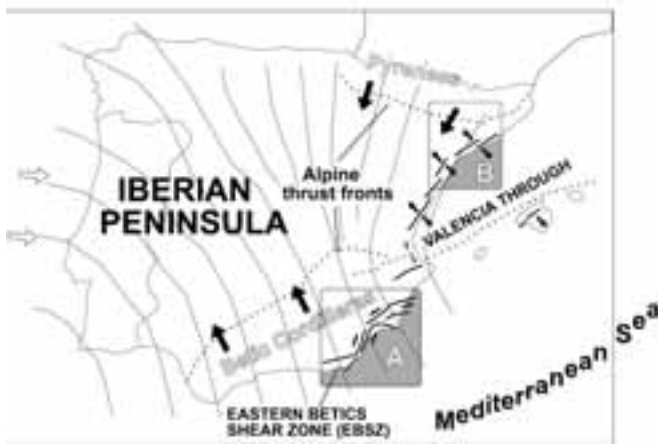


Figure 1 - Location of the tectonic zones to be visited during the field trip in the context of the alpine orogenic belts of the Iberian Peninsula and Neogene-Quaternary compressive stress field trajectories (dotted lines). Black arrows: Betic (Middle Miocene-Present) and Pyrenean (Paleogene - Early Neogene) compression; White arrows: Atlantic ridge push (late Cretaceous-Present). Zone A: Eastern Betics Shear Zone. Zone B: Catalan Coastal Ranges. In both boxes thin arrows indicate the sense of main tectonic displacements in the zones visited. Stress trajectories from Clothing et al. (2003) and Stich et al. (2003)

segment of the EBSZ, where coastal tectonics related to marine deposits and landforms of ISS 5 [explain this acronym] will be observed during the first day. Here we will follow along the central (Murcia) and northern (Alicante) segments of the EBSZ, exploring the geology and geomorphology of relevant (cortical scale) strike-slip fault zones and features related to their recent activity (trenching sites, seismites, fault travertines, etc.). After a half-day journey from

Alicante to Tarragona, the field trip will continue in the Catalan Coastal Ranges (CCR). Here, we will examine several aspects linked to normal faulting paleoseismicity, including fault-trenching sites

Both domains, the EBSZ and the CCR, are crustal-scale features linked to the Africa-Eurasia oblique convergence since the Neogene, but displaying different transpressive (EBSZ) and extensional (CCR) kinematics (Fig.1). Main sites to be visited deal with Quaternary deformations and paleoseismic features related to the activity of low slip-rate faults. However, this area displays a low-to- moderate instrumental seismicity, but it has been affected by significant (catastrophic) historical and/or pre-historical earthquakes. Seismic activity is characterized by small-magnitude earthquakes ($m_b < 4.5$) punctuated by occasional moderate-to-high-magnitude events ($> 5.0 m_b$).

In most of the cases present seismic activity is related to the well-known set of fault zones defining the different segments of the EBSZ and/or the CCR. Main fault zones to be visited are the Carboneras (CBF), Palomares (PLF), Lorca-Alhama de Murcia (LAF), Crevillente (CRF) and Bajo Segura (BSF) ones from south to north within the Almería, Murcia and Alicante regions (Figs. 2 and 3). They trace well-developed NE-SW to E-W faulted mountain fronts linked to strike-slip transpressive kinematics. Only in the BSF more discrete fold-limb scarps linked to blind faults substitute mountain fronts. Most of the mentioned faults are active faults and relevant historical earthquakes (MSK X -VIII) occurred within the area visited from 1522 up to the late 19th Century. Cities such as Almería, Vera, Lorca, Murcia and Torreveja were all destroyed and/or severely damaged during this span of time. The last notable earthquake in Spain also occurred in this zone, north of Lorca, the 5.0 m_b Mula event on 02/02/2002. However recent trenching studies carried out by the Complutense (Madrid) and Barcelona Universities has revealed the occurrence of strong Holocene seismic events on the LAF. (Figs. 3 and 4)

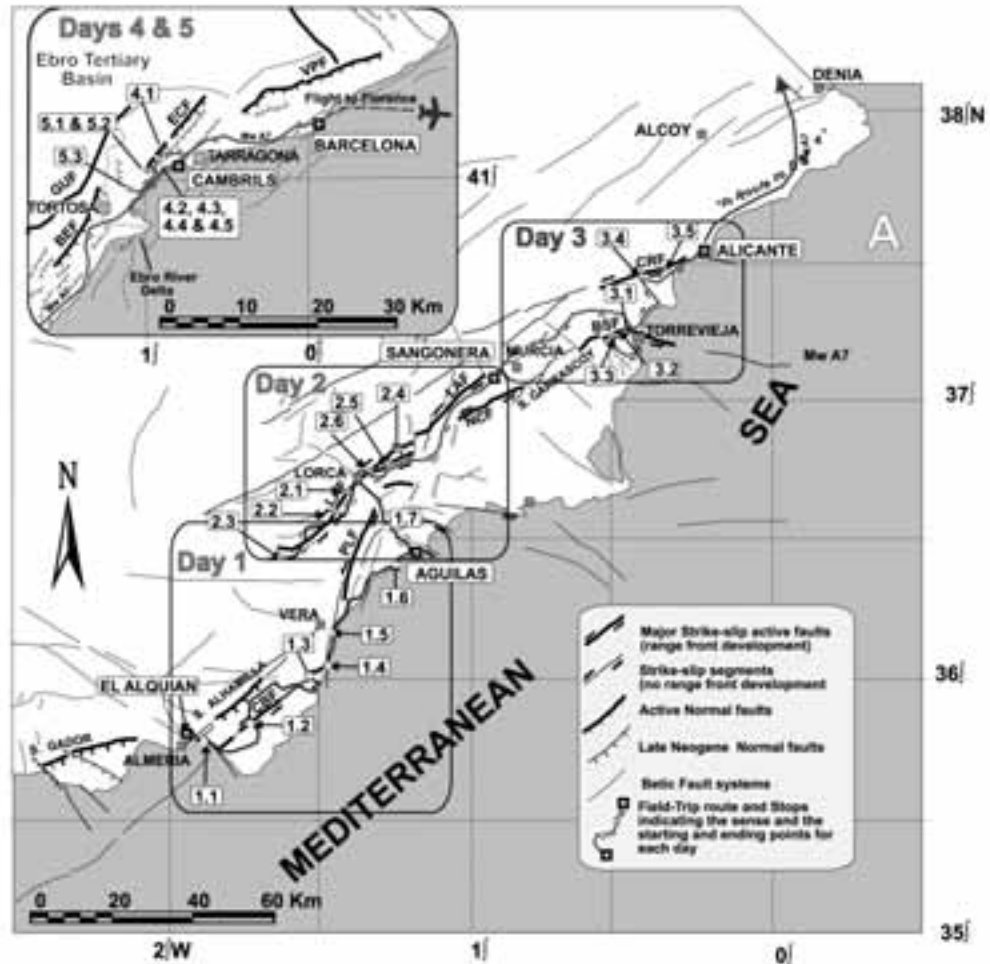


Figure 2 - Structural sketch of the Mediterranean sector of the Iberian Peninsula showing the itineraries and sequence of stops to be followed during the field-trip.

Travelling to the north, away from the Betic thrust front (Prebetic ranges), the degree of tectonic activity and present seismicity decrease. A relevant seismic gap occurs between the Pyrenean and Betic thrust fronts along the Valencian-Catalan coasts. Only some isolated and moderate events ($m_b < 4.0$) happen north of the Ebro River Delta, along the littoral sector of the CCR (Fig. 3). This fact corresponds to the occurrence of faulted mountain fronts linked to extensional tectonics. These range front faults have a broad NE-SW to NNE-SSW orientation, running subparallel to the coast. Among the different range front faults, the relevant one is the El Camp Fault (ECF) NE of the city of Tarragona, which will be the main objective of the

last stage of the field trip. Detailed trenching studies have been performed along this Quaternary structure by the University of Barcelona, supported and funded by ENRESA and the Spanish CNS research programs. In spite of the low seismicity of the zone, intensive research is justified by the presence of relatively old nuclear power plants at the end-zone of the Catalan Coastal Ranges.

Several guidebooks have been published for the zones of Almería, Murcia and Alicante on occasion of the National and International Congress held in SE Spain. These cover aspects complementary to those discussed in this field trip, and in some cases they deal with the same, and/or nearby outcrops visited

here. The most relevant ones are those published by Zazo et al., (1989: *2ª Reunión de Cuaternario Ibérico AEQUA-GTPQ*; 1998: *7th Int. Congress IAS*) and Martínez-Díaz et al., (2000: *V Congreso Geológico de España*). These geological guidebooks can be obtained upon request from the libraries of the universities of Madrid (UCM) and Alicante, and/or to the corresponding organising institutions (AEQUA, IAS, and SGE). In addition, the field-guide published by Blackwell Science focusing on the geology and geomorphology of the Almería Province (Mather et al., 2001) is also available. No complementary guidebooks are available for the Catalan Coastal Ranges. Map coverage of the daily

referenced to the corresponding 1:25.000 Maps. In the case of the Catalan Coastal Ranges, the most up-to-date 1:50.000 Map by the Institut Cartogràfic de Catalunya (ICC) has been used. The Geological Maps (1:50.000) of the region can be obtained from the Geological Survey of Spain (IGME). Map material can be consulted and purchased on the the following web sites: www.oan.es/servicios/GNIG.html (Instituto Geográfico Nac. -IGN-); www.icc.es (Institut Cartogràfic de Catalunya -ICC-); www.igme.es/internet/itge.htm (Instituto Geológico y Minero de España -IGME-); and www.tiendaverde.org (Commercial Map Site).

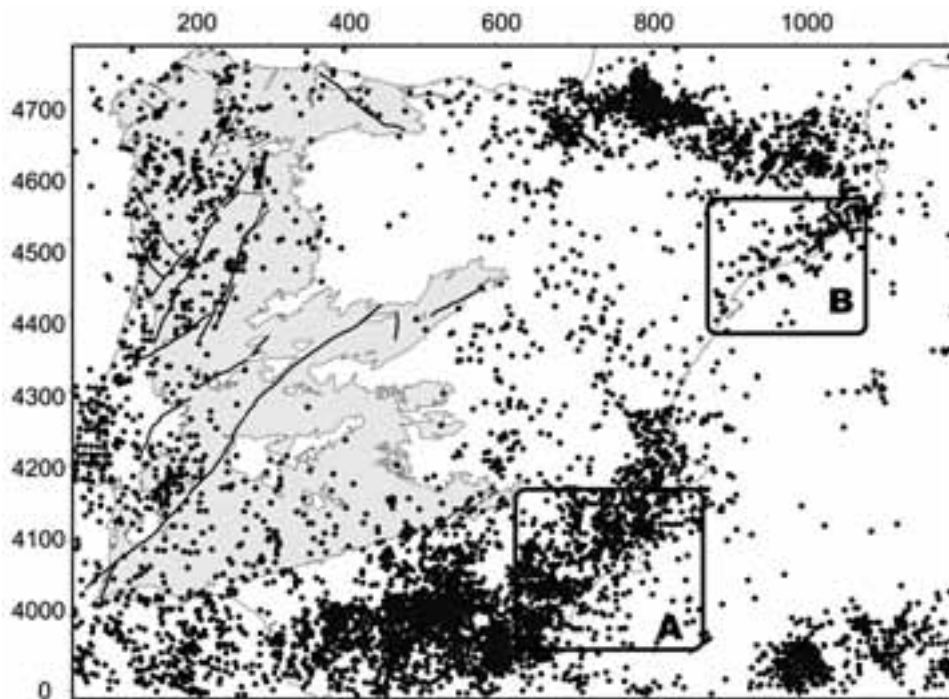


Figure 3 - Present-day seismic activity of the Spanish Mediterranean sector (on-line information at <http://www.geo.ign.es/servidor/sismo/cnis>)

itineraries can be obtained from many of the different series of topographic maps published in Spain. The most complete ones are the 1:50.000 Series of the “*Mapa Militar de España*” published by the “*Servicio Geográfico del Ejército*” (SGE). But for detailed information, the new 1:25.000 Series edited by the “*Instituto Geográfico Nacional*” (IGN) are the best maps. All the stops on this fieldtrip have been

Regional geologic setting

P.G. Silva, E. Masana, P. Alfaro, J.J. Martínez-Díaz and T. Bardají.

The Betic Cordillera constitutes the westernmost segment of the Mediterranean Alpine fold and thrust belt developed in response to the NNW-SSE Cenozoic Africa-Eurasia collision, with a relative velocity of

between 4 and 5 mm/yr. The direction of convergence has remained constant for at least the last 9 million years (Late Miocene - Present), as inferred from plate kinematics, and from the analysis of palaeostresses. It is located in southern Spain and presents a largely ENE-WSW orientation (Fig. 1).

The mountain belt is divided into two main zones, an unmetamorphosed External Zone to the north and a metamorphic Internal Zone to the south (Fig.4). The External zone is formed by the Subbetic and Prebetic zones, which are mainly composed of Mesozoic (Jurassic and Cretaceous carbonates) and Tertiary sedimentary rocks. The internal zone of the Cordillera consists of a thrust stack with three

schists, mica-schists and quartzites. Some authors consider the lowest Permo-Triassic materials of the Alpujarride Complex (sometimes detached) as another independent tectonic unit (the Almagrider Complex). The Maláguide Complex is the highest unit and is generally unmetamorphosed, consisting of Permo-Triassic red beds and Jurassic limestones and dolomites topped by an overthrust Tertiary sequence of Eocene-Miocene age (Lonergan, 1993).

The main compressional deformation occurred during the Neogene, but in the Internal Zone deformation and metamorphism developed from the Eocene to the Early Miocene with earliest nappe emplacement occurring at about the Eocene-Oligocene transition (Sanz de Galdeano, 1990). Compressional deformation migrated to the north during the Miocene, making room for the thin-skinned thrusting and folding of the External Zones (Banks and Warburton, 1991). In the Central Sector of the Betics, the extensional collapse of the Cordillera started during Late Oligocene-Miocene transition, culminating with the opening of the Alboran Sea (Platt and Vissers, 1989; Galindo Zaldívar et al., 1999).

The eastern sector of the Betic Cordilleras has been subjected to mountain building up until the middle Miocene. Afterwards, strike and oblique-slip

tectonics dominated, and contrasting transtensive and transpressive kinematics occurred from the Tortonian to the Pliocene, followed by substantial Plio-Quaternary uplift. The present configuration of the zone is mainly linked to one of the more prominent post-collisional crustal-scale structures of the Cordillera, the so-called Eastern Betics Shear Zone (EBSZ: Larouzière et al., 1988; Silva et al, 1993). The EBSZ constitutes a left-lateral shear zone of sigmoidal geometry, stretching from Almería to Alicante over more than 450 km (Fig. 5). This is a NE-SW trending morpho-structural feature overprinted, but locally accommodated, on the ENE-WSW to E-W grain of the Cordillera consisting of the previous

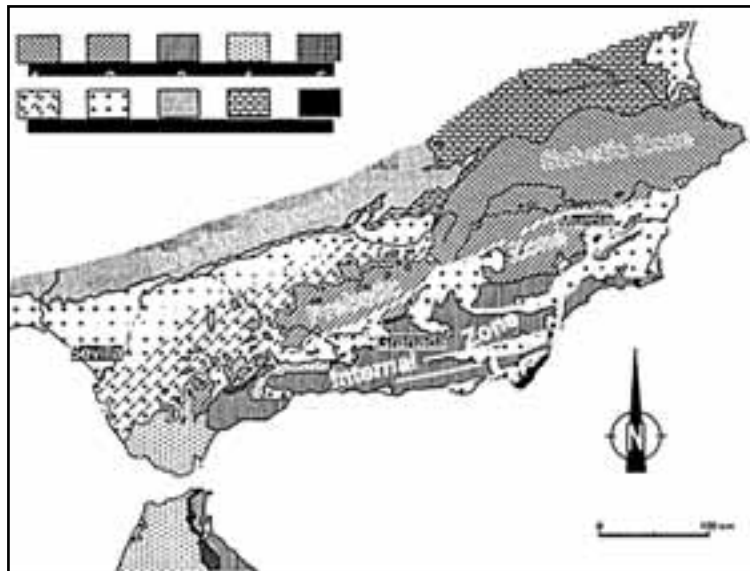


Figure 4 - Geological map of southern Spain showing the structure of the Betic Cordillera. 1: Prebetic zone; 2: Subbetic zone; 3: Internal (Betic) zone; 4: Gibraltar Flysch units; 5: Betic Dorsal; 6: Olisthostrom units; 7: Neogene-Quaternary basins; 8: Paleozoic Substratum (Iberian Massif); 9: Thin-skinned mesozoic materials (Iberian Chain); 10: Neogene and Quaternary Volcanics. Modified from Fontboté and Estévez (1980).

tectonic units: the Nevado-Filábride, Alpujarride and Maláguide complexes. The Nevado-Filábride Complex is the lowest unit and exhibits high-pressure - low temperature metamorphic facies (i.e., Green Schist and Amphibolites). The overlying Alpujarride Complex displays a sequence of low-medium metamorphic facies, predominantly

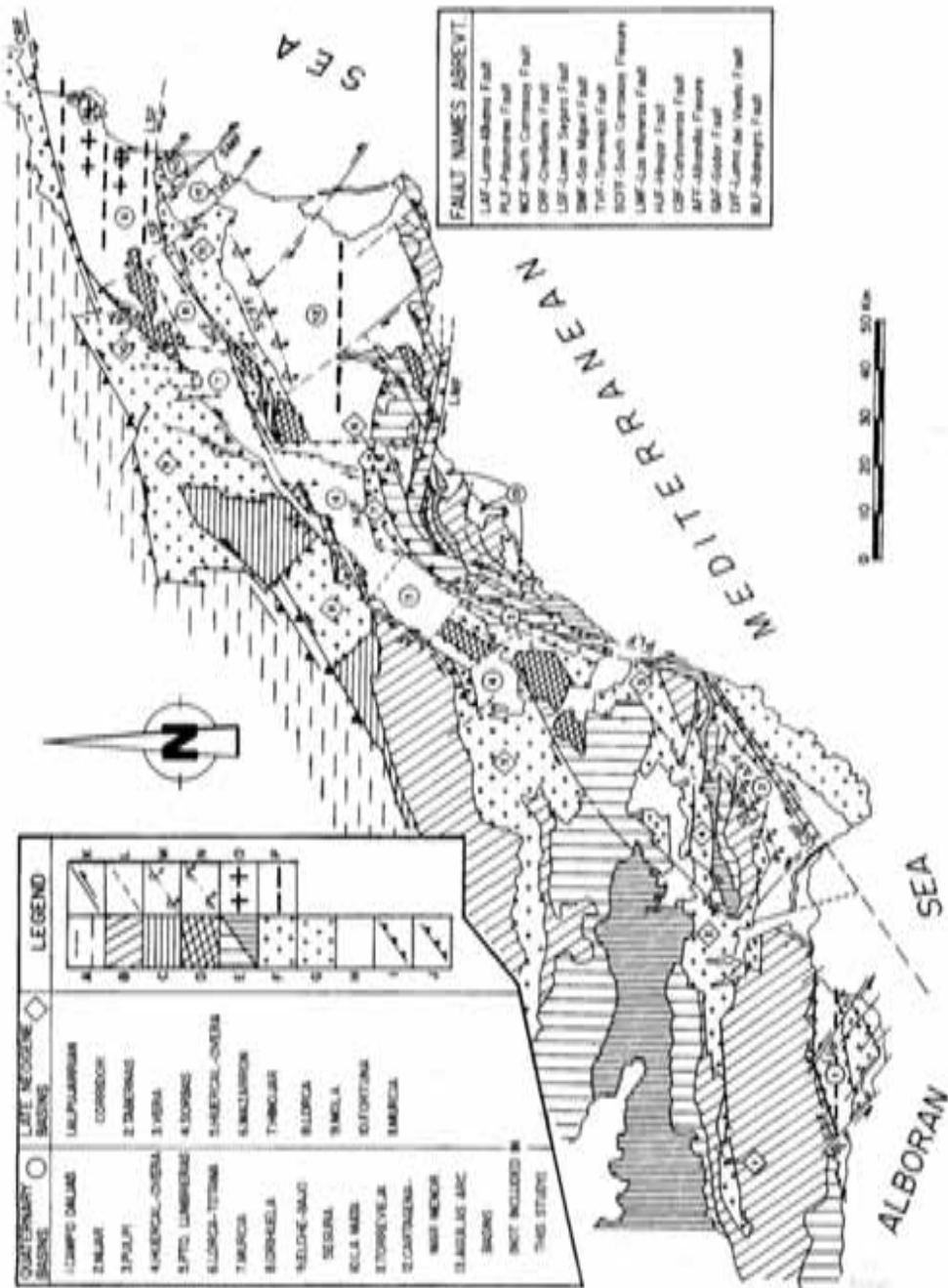


Figure 5 - Geological and Structural map of the Eastern Betic Cordillera. A: External Betic zone; B: Alpujarride Complex; C: Maláguide Complex; D: Almagrde Complex; E: Nevado Filábride Complex; F: Neogene basins; G: Late Neogene volcanics; H: Quaternary basins; I: Normal faults; J: Reverse faults; K: Strike-slip faults; L: Buried (geophysical) faults; 0: Anticline/ Uplifting axis; P: Syncline / subsiding axis. After Silva et al., 1993.

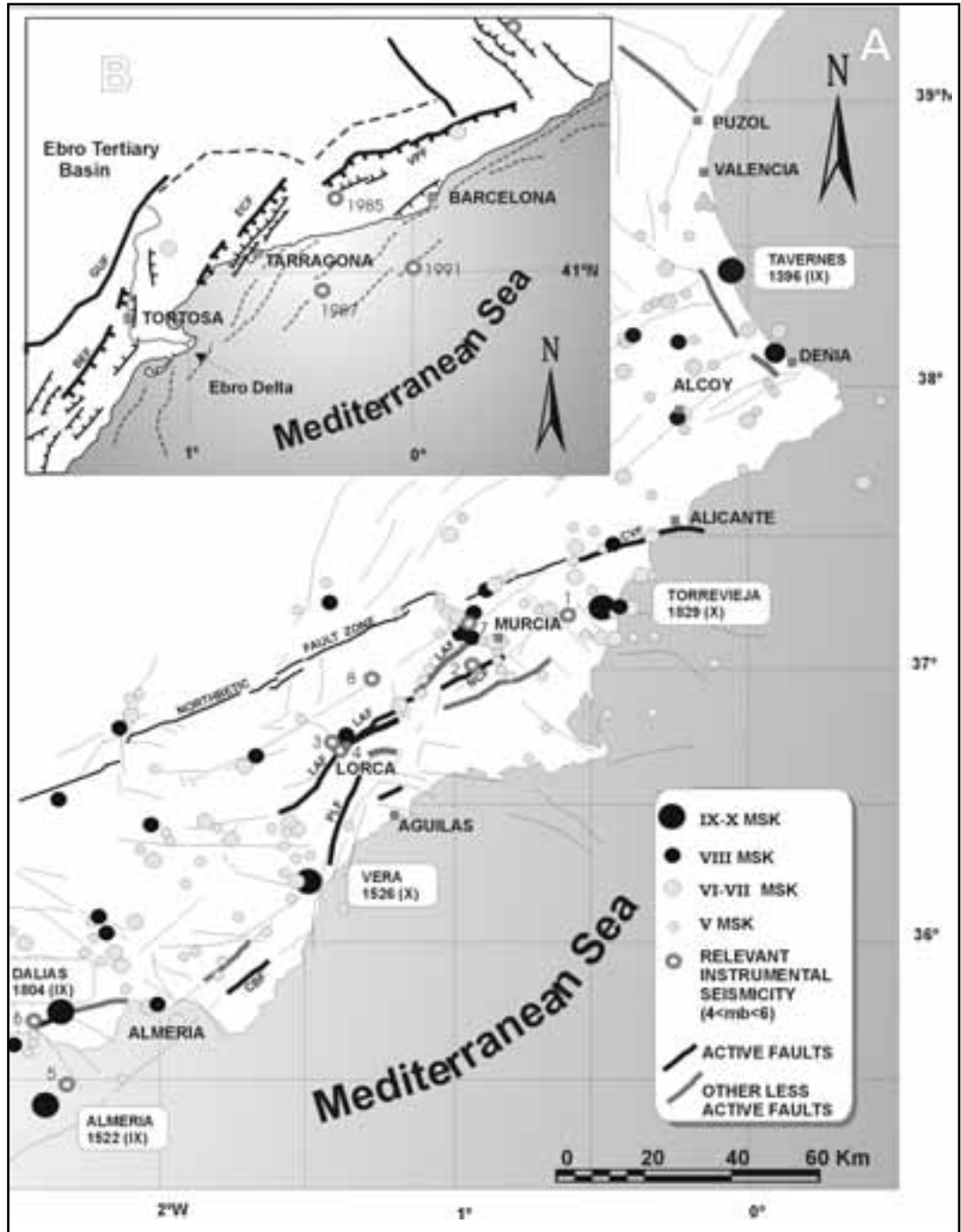


Figure 6 - Seismic activity in the Mediterranean sector of Spain showing historical (I_0) and instrumental (I_{max}) earthquakes with intensities of up to IV MSK. Numbered circled points indicate the location of the instrumentally recorded events with magnitudes (m_b) up to 4. (1) Jacarilla 1919: 5.1; (2) Sangonera 1946: 4.3 (3) Lorca 1977: 4.2; (4) Lorca 1978: 4.3; (5) Adra 1995: 5.2; (6) Adra 1996: 5.0; (7) Alcantarilla 1995: 4.1; (8) Mula 1999: 5.0; (9) Lorca 2000: 4.0. After Silva et al 2003 and Masana, 1996

Betic thrust planes and folds. This tectonic corridor is defined by the well-known set of the Betic Cordillera post-orogenic, NE-SW left-lateral strike-slip faults initially classified by Bousquet and Montenat (1974), Bousquet and Phillip (1976) and Bousquet (1979).

Late Neogene activity of this transcurrent zone gave rise to intense magmatic phenomena and strike-slip basin formation (Montenat et al., 1987). Neogene basins evolved along both sides of the present corridor (Fig. 6), in which ancient Betic paleomassifs, mainly comprised of Almagrde materials were located (Larouzière et al., 1988). All these basins evolved from open marine conditions during the Tortonian to progressive shallow marine, littoral and continental environments in the Late Pliocene-Early Quaternary. Starting from this span of time a stress field rotation from N170 to N150 triggered substantial uplift (>250m in some zones) as well as a generalised episode of inversion in the former Neogene basins, most of which are visible in the present-day contour of the zone (Montenat et al., 1987; Silva et al., 1993). Later, during the Early Quaternary, the reestablishment of the compressive stress to the N170 orientation triggered relevant changes in fault kinematics, modifying the location and geometry of the sedimentary zones. The development of the present landscape started in this last period, giving rise to the formation of sedimentary troughs (i.e. the Guadalentín Depression and the Bajo Segura Basin) in areas previously occupied by ancient Betic paleomassifs.

The **main faults controlling the EBSZ**, (i.e. PLF and LAF) record important accumulated left-lateral slip (8 to 20 km) from the Messinian to the present (Weijermars, 1987; Larouzière et al., 1988) working as the principal displacement zone of the EBSZ (Silva et al., 1993). Both faults mark where the Guadalentín Depression gives room to the development of prominent mountain fronts, as well as displaying different characteristic features of active strike-slip faulting (offset channels, spur ridges, fault travertines, etc., Silva et al., 1992; 2003). To the east, the emerged sector of the Aguilas Arc was mainly dominated by a transpressive tectonics during its late Neogene emplacement (Coppiet et al., 1990), and, since the Pliocene, by the backward gravitational collapse of the structure along the ancient Betic thrust planes. Two additional tectonic domains develop in the ending-zones of the EBSZ: the Southern (Almería) and Northern (Murcia-Alicante) terminal splays

(Silva et al., 1993). The Southern terminal splay is controlled by the well-known NE-SW Carboneras (CBF) left-lateral strike-slip fault (Weijermars, 1987; Keller et al., 1995; Faulkner et al., 2003), but also by the Gador (GAF) and Southern Alhamilla (AAF) faults (Fig.5). In these last two strike-slip faulting is associated with extensional kinematics triggered by the post-orogenic gravitational collapse of the Betic Cordillera, and/or block tectonics driven by the regional compression (Martínez-Díaz 2001). In contrast, the Northern Terminal Splay, is controlled by the Crevillente (CRF) and Bajo Segura (BSF) faults, in which mainly transpressive kinematics have occurred since the Late Miocene (Silva et al., 1993; Alfaro et al., 2002a, b). Blind reverse faulting and fold-limb scarps are common in this terminal splay, and onshore structures extend offshore into the Mediterranean Sea (Alfaro et al., 2002b).

Regional studies (Buforn et al., 1990; Sanz de Galdeano et al., 1995) indicate the occurrence of a small-medium magnitude (<5 mb) instrumental seismicity, generally shallow (<11km), distributed along the outline of the EBSZ (Fig. 6a). Only a few events (Fig. 6) have reached or surpassed the cut-off of mb 4.0. As illustrated by these events, magnitudes of 5.0 mb are sufficient to generate maximum intensities of VII MSK in the soft sedimentary filling of Quaternary basins. Lower magnitudes – those between 4.0 and 4.5mb -- are characteristic of VI MSK. Despite these distinct seismic limits, the historical record indicates the occurrence of strong events, up to VII MSK in the eastern Betic Cordillera --among them, five of Spain's top-ten most destructive earthquakes (>IX MSK) (Fig. 6a). In some of them (i.e. the 1829 Torreveja Earthquake) maximum magnitudes have been estimated as ranging between 6.5-7.0.

As displayed in Figure 6, most of the strike-slip faults are segmented into different mountain fronts. Some of these have been classified as active (Class 1) range-front faults on the basis of their morphometric properties and faulting evidences, in all cases with related uplift rates of over 0.08 m/ka (Silva et al., 2003). Some of them are clearly related to present-day seismicity, as is the case of the GAF, CRF, NCF, and especially the central segment of the LAF. In contrast, some individual active fronts display an unforeseen aseismic character, as is the case of the CBF, PLF and the southern segment of the LAF south of Lorca (Silva et al., 2003; Martínez-Díaz, 1999).

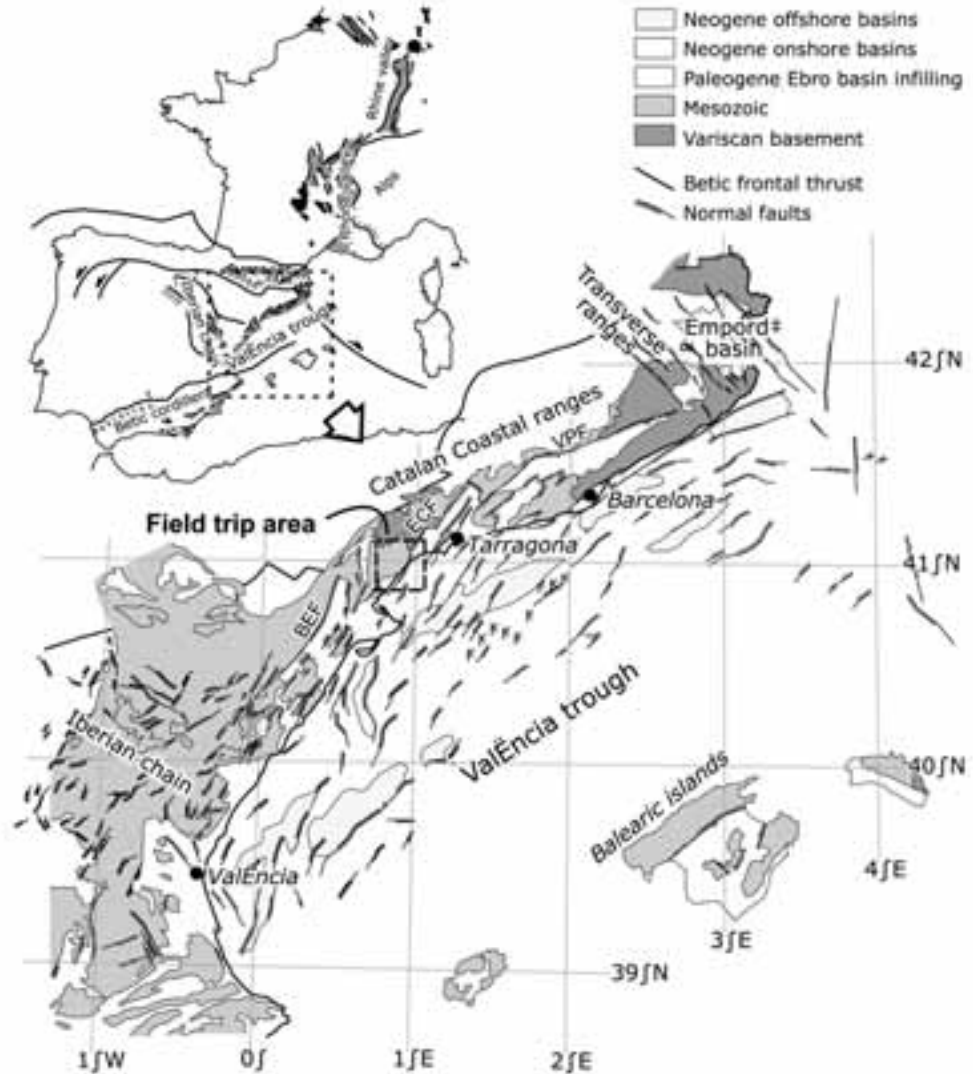


Figure 7 - Simplified map of the northwestern margin of the València trough, based on Roca (1992) and Roca and Guimerà (1992). VPF: Vallès-Penedès fault, ECF: El Camp fault, BEF: Baix Ebre fault.

Instrumental seismicity seems to be spatially related with the activity of smaller NW-SE and NE-SW faults (Martínez-Díaz et al., 2001). The recurrence interval for the seismic activity at these faults is shorter than that of the major fault zones, due to a smaller cycle of stress accumulation. The seismicity of the past 100 years therefore gives a better record of smaller seismogenic fault activity. However, earthquake nucleation seems to be preferentially focused at major bends, or intersections, of the main NE-SW strike-slip fault zones with subsidiary NW-SE fault

systems, where a major accumulation of stress is expected (Fig. 8). In this sense it is necessary to note that the strongest earthquakes ($I_0 > VIII$ MSK) felt in SE Spain are recorded at major inflexion points of the EBSZ, as is the case of the 1518 Vera, 1522 Almería and 1829 Torrevejea earthquakes (Fig. 8).

In detail, earthquake nucleation at relevant fault trace bending is significant at the segment boundary between the southern and central segments of the LAF at Lorca (Silva et al., 2003), where three VIII

MSK events (years 1579, 1674 and 1818) have occurred. In this same zone, two recent 4.2 (1977) and 4.3 mb (1978) have occurred (Mezcua et al., 1984) producing minor damage (Martinez-Díaz 2000; Martinez-Díaz et al., 2002). Earthquake nucleation at fault intersection is also relevant where the LAF tapers out at its intersection with the Segura Valley Fault zone in Alcantarilla (Murcia), or at the intersection of the Loma del Viento Fault with the Gador range-front fault (Almería) at Campo Dalías (Fig. 6a). In the first case (Alcantarilla) notable earthquakes have been produced in both the past and recent times, for example, the 1911 Torres de Cotilla and Lorquí VII MSK events, and the 4.1mb 1996 Alcantarilla event. In the second case (Campo Dalías) more important seismic events have been recorded, as is the case of the 1804 Dalías IX MSK event, but also the recent 1995-1996 seismic sequence of Adra with a maximum 5.2mb event, which seems to be related to similar NW-SE transverse faults.

Recorded seismic activity indicates that active fault (Class 1) fronts ($> 0,08\text{m/ka}$), can record isolated seismic events as large as IX MSK (Gador), but, generally VIII-VII MSK intensity with recurrence intervals ranging from c.a. 100 to 250 years is the common behaviour for the last 650 years in SE Spain. This behaviour can be illustrated by the seismic activity released during the theorised long recurrence intervals of strong paleoseismic events, bracketed within 1,750-2,600 years for minimum slip conditions, and within 10,000-12,500 years for maximum slip conditions (Silva et al., 2003). In any case, an overall aseismic character is displayed by some of the Class 1 fronts, as is the case of CBF, PLF and the southern segment of the LAF. In these fronts, aseismic fault creep, as suggested by Carreño et al (1989), Silva et al. (1997; 2003) and Faulkner et al. (2003) may help to maintain Class 1 features. Less active (Class 2) range-fault fronts (ca. $0,07\text{-}0,03\text{m/ka}$) only exhibit historic events as large as V MSK intensity and exceptionally larger, but isolated, VII-VI MSK events, as is the case of the northern segments of the LAF. No data about paleoseismicity are available for this type of fronts, but surface rupture events with intermediate recurrence intervals of 12,500-25,000 years could be theorised from uniform slip fault models (Silva et al., 2003).

The Catalan Coastal Ranges are located at the emerged easternmost part of the Valencia Trough, a NE-SW trending Cenozoic basin, located in the

western Mediterranean between the Iberian Peninsula and the Balearic Islands. The Valencia Trough is a part of the intraplate rift that crosses Western Europe, in a roughly north-south direction, from the North Sea to the southern Western Mediterranean Sea, passing through the Rhine and Rhone valleys and the eastern margin of the Iberian Peninsula. The northwestern part of the trough (the Iberian margin) is characterized by normal faulting, partly affecting up to Upper Miocene and Plio-Quaternary rocks, whereas the southeastern part (the Balearic margin) is formed by a thrust belt affecting middle Miocene strata, which correspond to the external Betics. This asymmetry is also reflected in the extremely thinned crustal structure (Banda and Santanach, 1992).

Along the Iberian margin the Paleogene contractional structures have been overprinted by an extensional fault system, which [?]changes progressively from ENE-WSW in the northeast, to practically N-S in the south, describing an arc parallel to the coast (Fig. 7). Along the Catalan Coastal Ranges (CCR), the emerged part of the Valencia Trough margin occupies a narrow zone (around 25 km wide) clearly limited to the NW by an *en echelon* array of major faults. To the south, the distribution of the emerged faults is over 100 km wide. An important part of these normal faults results from negative inversion of Paleogene thrusts or strike-slip faults since the late Oligocene (Roca, 1996). However, post-rifting thermal subsidence has characterized middle and late Neogene times. A poorly-differentiated alkaline volcanism occurred in this extensional structure from middle Miocene to Recent (Martí et al. 1992). The Neogene activity of the faults in the CCR generated several NE-SW elongated basins, from north to south: the Vallès-Penedès, El Camp and El Baix Ebre basins. The thickness of the Neogene sediments filling these basins decreases from north to south (4000 m in Vallès to 400 m in Baix Ebre).

Depthwise, this extensional fault system has a listric geometry and joint into a detachment level at 13-15 km. This detachment level coincides with the Moho depth in the axial area of the trough, although in the marginal areas it is located in an upper crustal position. Locally, shallower horizons of detachment occur, both in the Mesozoic cover (Upper Triassic) and in the Variscan basement. The ESCI-València Trough deep seismic reflection profile crosses this extensional fault system. It shows a reflective lower crust containing an anastomosing shear zone, into

which the normal faults vanish. (Sàbat et al., 1995). This deep shear zone matches the detachment level at 13 km depth described by Roca and Guimerà (1992) and Gómez and Guimerà (1999). Thus the deep extensional detachment corresponds to the reactivated sole thrust of the Paleogene contractional thrust system.

A moderate to low seismic activity occurs along this rifted megastructure in Western Europe, although some strong earthquakes happened in historical times causing significant damage as well as casualties. The Basel earthquake of 1356 (Vogt, 1979) is a well-known example of such events. Along the Iberian margin, the strongest historical earthquakes are those of the Catalan seismic crisis of the 15th century (1427-28, $I_0 = IX$), and the 1396 AD Tabernes and 1748 AD Énguera events (both of $I_0 = IX$). Each of these earthquakes was caused by different faults. Thus, no fault has produced two large earthquakes in historical times (the last 700 yrs). This is due to the slow slip-rate of these faults, which show recurrence periods for their maximum earthquakes in the order of ten times larger than the historical record.

At the northwestern margin of the Valencia trough only four earthquakes with $I_0 \geq IX$ (and seven with $I_0 \geq VIII$) occurred over the seven centuries covered by the record. During instrumental times, the maximum earthquake reached a magnitude of $m_b = 5.1$, and only 15 earthquakes showed magnitudes $m_b \geq 4.0$. Along the CCR the seismicity is noticeable between the Transverse ranges and Barcelona for the historical period, but reaches Tarragona in the south during instrumental times. The area between the cities of Tarragona and Valencia can be considered a seismic gap (silent area) showing very few events, and these being of the lowest magnitudes and intensities.

In any case, the CCR zone has undergone moderate activity recently, as evidenced by structural, geomorphological and paleoseismological studies (Masana, 1995, 1996). The active tectonic indicators are mainly concentrated in the southern part of the ranges. Mountain front analysis (sinuosity, basin shape, concave profiles across the front, faceted spurs, gradient index anomalies, drainage network distribution) revealed that the most recent activity is at the Montseny (north of the Vallès-Penedès fault), El Camp (southern segment), Plà del Burgar, and Baix Ebre fronts.

The detection of a number of fault scarps affecting Quaternary alluvial fans triggered the first paleoseismological studies along the El Camp fault (Masana 1995, Santanach et al., 2001). These concluded that the El Camp fault is seismogenic, even though it's been seismically silent during the historical period, as shown by the absence of any significant earthquake in the historical seismic catalogue of the region. A detailed morphological and trenching analysis along the El Camp fault revealed that the slip-rate of the fault is low (0.02 mm/yr), but presents geological evidence of three past earthquakes, suggesting a long mean recurrence period (30 ka) and a short elapsed time (ca 3000 yrs). The maximum magnitude estimated for this fault was Mw 6.7.

Field trip itinerary

DAY 1

The Almería Region: The Carboneras And Palomares Strike-slip Fault Zones

T. Bardají, P.G. Silva, J.L. Goy, C. Zazo and K.Reicherter

This first day introduces the geodynamic framework of the southern terminal splay of the EBSZ, and explores the geology and geomorphology of two of the better-known strike-slip fault zones of this area: The Carboneras (CBF) and Palomares (PLF) left-lateral faults. Originally described by Bousquet and Phillip (1976), they have been re-visited time after time for geomorphological, Quaternary chronology and neotectonics studies (Goy and Zazo, 1984, 1986; Bell et al., 1997), structural analyses (Bousquet, 1979; Coppier et al., 1990; Keller et al., 1995; Faulkner et al., 2003) and geophysical GPR research (Reicherter and Reiss, 2001).

Transfer to Stop 1.1: Leaving El Alquian on the N344 (heading towards Cabo de Gata) turn left onto the AL-202. After the town of Retamares we come into Cabo de Gata Natural Park. After the park's signpost turn right onto the first paved road to the coast. upon reaching the Torre Garcia ruins, turn left and take the road (suitable for coaches) down to the Rambla floor. Leave the car/coach at the beach-parking lot and walk upstream along the right bank of the rambla until the ancient Roman well

Stop 1.1:

Torre García – Rambla de las Amoladeras

(1:25.000 Map Cabo de Gata, IGN Series).

At this point the coastal termination of N40-60 strike-slip faults can be observed (subparallel to CBF –Fig. 1.1) affecting beach deposits deposited between 180 and 100 ka (OIS 7 – OIS 5). A subvertical-cemented fault plane exhumed along the right bank of the rambla marks the fault route, and controls the present elevation of the littoral deposits at both sides of the

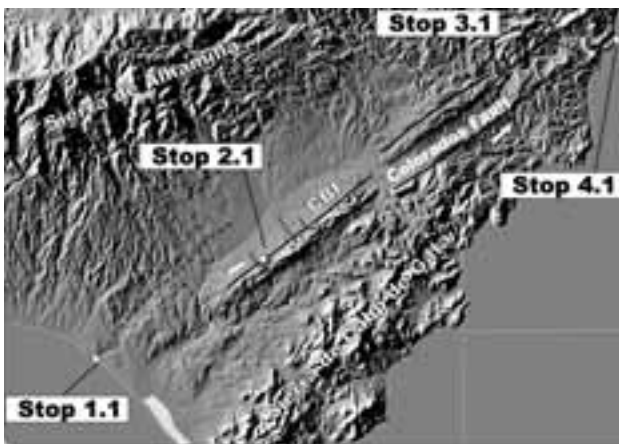


Figure 1.1 - Digital elevation model of the Almería region showing the locations of stops 1-1 up to 1-4 within the Carboneras Fault Zone. Note drainage anomalies in the La Serrata range front fault..

rambla. Additional N140-160 normal flexures assist beach progradation and uplift from OIS 7 to OIS 5. In addition, this site is one of the most complete and well-dated *Strombus bubonius*- bearing marine sequences of SE Spain, allowing the establishment of the Late Quaternary stratigraphy and sea-level changes from the earlier works of Goy and Zazo (1983; 1986).

A first observation from the left side of the rambla will allow us to get a panoramic view of the whole sequence. The sequence consists of at least four offlapping prograding marine units (Figure 1.2), separated from each other by dune systems or erosional surfaces. Three of these marine units contain *Strombus bubonius*, the main representative of the warm “senegalese” fauna that entered the Mediterranean during the middle-late Pleistocene. The first entry of this warm fauna into the Mediterranean occurred as early as OIS 7, experiencing a massive expansion during ISS 5e, and surviving in some privileged sites (such as Almería) during the whole

interglacial (Hillaire-Marcel et al., 1986; Goy et al., 1986; Zazo and Goy, 1989; Zazo et al., 2003). This outcrop is one of the first where this assumption could be proved by dating mollusc shells, since confirmed by dating corals from other Spanish sites more recently (Zazo et al., 2003).

The three *S. bubonius*-bearing units outcropping on the right margin of the rambla correlates, by U-series dating, with ISS 7a (180 ka), ISS 5e (128 ka) and ISS 5c (95 ka), and they are separated from each other by erosional surfaces with beach features and evidence of early cementation. The maximum heights at which these units stand at present is +15m (7a), +11m (5e) and +8m (5c). These units represent highstands of sea level during the corresponding interglacials, while the erosional surfaces represent the intervening glacial lowstands. Sedimentologic analyses allow us to distinguish the transition between foreshore and shoreface environments, that is, datum level for each of the dated beaches. In order to calculate the uplift rate of this area, we have taken the ISS 5e as the reference level. The position of sea level during this substage has been measured in tectonically stable areas at +2m above present sea level, although a rapid ingressión before the close of the substage seems to have brought the sea level up to +6m asl. Consequently,

the uplifting trend calculated for this area is around 0.07mm/yr.

The sequence is affected by N40-60 strike slip faults (subparallel to CBF), which also condition the present outline of the coast. A subvertical-cemented fault plane exhumed along the rambla bank, marks the fault trace and controls the present elevation of the littoral deposits at both sides of the rambla. Additional N140-160 normal flexures assist beach progradation and uplift from OIS 7 to OIS 5.

Transfer to Stop 1.2: Coming back to the AL-202 from Torre Garcia turn to the east (Cabo de Gata). After crossing the Rambla Amoladeras head towards Ruescas-San Jose, driving along the north wall of the “Michelin” research facilities until the next intersection. There turn left (north) onto the AL-206, heading towards Nijar. La Serrata Fault-Ridge appears on the horizon. Cross the range and just

before the road leaves the Ridge park at the second curve (on your right). Coaches will have to continue down the slope of the alluvial fan systems until the main rambla, then turn the vehicle around going back up the road until the second curve, and parking on the right. Walk up toward the top of the ridge, this is stop 1.2: a pressure-ridge of the Carboneras Fault. Note at the summit a bench-mark for the geodetic levelling of potential present fault displacements.

Stop 1.2:
Sierra de La Serrata Mountain Front:
Carboneras fault.

(1:25.000 Map Fernán Pérez, IGN Series)

From this vantage point it is possible to observe the alluvial slope of the La Serrata Mountain Front, the southern segment of the Carboneras Fault. The piedmont is made up of three well-developed alluvial fan systems. The oldest one has a strongly-developed calcrete crust about 1 m thick. At present they only appear as irregular, beheaded remnants, buttressed against the fault-front in inter-fan upper-slope locations. The main piedmont slope is formed by Upper Pleistocene alluvial fan surfaces supporting 10YR argilic (Bt) soil horizons with secondary carbonate accumulations (Bell et al., 1997). These are proximally trenched, but active distal aggradation occurred during the Holocene at the basin centre. In all cases, these alluvial fans only have a single feed-channel, characteristic of tectonically active mountain fronts. The range front is controlled by the sinistral strike-slip Carboneras fault along a total length of 14.9 km following a broad N52 strike (Fig. 1.1), and displays the lowest sinuosity index (Smf) of SE Spain (1.17). This fault has an accumulated horizontal offset estimated to be ca 40 km, mainly produced between 18 to 5 Ma ago (Messinian), yielding slip rates of ca 2.7 mm/yr. Only minor displacements have been attributed to Quaternary

times. However, reverse slip pushed up the Neogene volcanic rocks over the Pleistocene deposits. In many places the transpressional kinematics gave place to positive flower structures, which occasionally involved Messinian gypsums and marls, giving rise to prominent linear pressure-ridges. These are the most characteristic tectonic landforms of this faulted mountain front displaying typical widths of 50-60m and relative heights of 40-90m. We are now standing on one of these pressure-ridges. If we turn around to look at the range front, it is possible to observe a close to 90-degree deflection of a little creek along the Carboneras Fault trace, which is another noticeable characteristic of the southern segment of this fault. The stream parallels the fault zone for some 150m before exiting the pressure ridge onto the piedmont alluvial fan. The left-lateral stream offset has been estimated to be at least middle Pleistocene (ca 500 ka BP) in age, but there is a lack of evidence for significant, more recent (Late Quaternary) horizontal slip (Bell et al., 1997). In contrast, moderate vertical slip (5-10 m) has occurred over the last 200 ka, as reported in coastal locations at the southern (i.e. Stop 1.1), and northern fault terminations (Goy and Zazo, 1986; Bell et al., 1997).

Rates of vertical uplift in these zones have been suggested as being 0.1 to 0.05 mm/yr. GPR data at these zones also reveals similar rates (Reicherter and Reiss, 2001). This southern segment of the fault is "aseismic", as shown by micro-seismicity surveys. Only a rather distributed, weak seismicity ($M < 2.5$) can be presently found at its northern segment (Keller et al., 1995; Faulkner et al., 2003). The latter authors propose that aseismic fault creep within the phyllosilicate-rich fault gouge may occur punctuated by larger events (ca M6) nucleated within more resistant Betic substratum blocks (i.e. dolomites) in its northern segment. This mechanism would explain

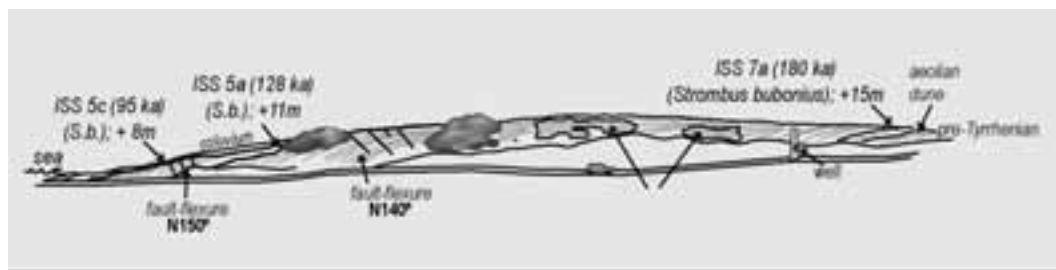


Figure 1.2 - Sequence of *Strombus bubonius*-bearing marine units outcropping at the right margin of Rambla Amoladeras (Almería, SE Spain), (after Zazo et al., 1998).

the occurrence of the destructive IX MSK Almería Earthquake (1522 AD).

Transfer to (en route) Stop. 1.3: If in coach go back along the AL-206 (towards San Jose) until the next roundabout (Los Albaricoques junction), go around it and head towards Nijar. Take the N-340 Motorway (toll-free) towards Murcia (North) and continue on it until the Carboneras Exit (at Venta del Pobre). Follow N341 and at the Village of Carboneras follow the signs for coastal road AL-118 (towards Aguilas). After descending el Collado de La Granatilla (a relevant viewpoint), just before the Rambla de los Moros bridge, park the vehicle on the right as you come onto this ancient road. You now get a superb view of the multi-coloured badlands developed in the Carboneras Fault gouge. If convenient, a small pathway descends to the fault outcrop from the old road.

Stop 1.3 (en route):

The Carboneras Fault Gouge at Sopalmo.

(1:25.000 Map Agua del Medio, IGN Series).

The northern segment of the Carboneras Fault zone has been subdivided into different subparallel faults, the Polopos, Sopalmo and Colorados (Keller et al., 1995). These faults are separating the Cabo de Gata volcanics to the SE from the Sierra de La Cabrera schists to the NW, along a NE-SW trend (Fig 1.1). From this viewpoint we can identify the Colorados Fault gouge (cover photo). This is exposed as a series of individual gouge-units 4-5 m wide, containing a range of cataclastic and mylonitic features. Materials incorporated in the fault zone include Burdigalian marls, volcanic rocks (calcalkaline andesites), Triassic phyllites and foliated mica-schist (exhumed phyllosilicate-rich fault gouge). Fault uplift has been useful in controlling drainage development in this sector. Looking towards the village of Sopalmo, a thick unit of “fluvial gravels” can be observed above visible road cutting. The village is located in a hill between the (NW-SE) Rambla de Los Moros and the larger Macenas Rambla Valley, which drain towards the NE. These gravels, now located in the headwater of the Rambla de Los Moros, were deposited by the Macenas one. The incorporation of these fluvial deposits into this shorter drainage basin that developed transverse to the CBF illustrates an active process of river capture due to continuous uplift (Harvey et al., 2001). If suitable, vehicles can park opposite the Sopalmo Bar at the village and go down to explore the fluvial gravels at the roadcut.

Transfer to Stop 1.4: Continue along the AL-118 and drive down the Macenas Rambla valley, which follows along the Polopos fault. En route notice the two Quaternary terraces exposed downstream from the rambla bridge. Continue to where the road meets the coastline. Coaches can park on the right-hand road-shoulder beyond the intersection. Cars can take the road marked “Playa de Macenas”. Minibuses and/or vans have to park next to the Beach-Bar



Figure 1.3 - Geomorphology and structural elements outcropping between Torre de Macenas (North) and the Punta del Peñon Watchtower (South), where the CBF and PLF systems intersect. Inset detail of PLF striations adjacent to the watchtower.

“Obscure” and then walk south along the coast road until the Punta del Peñon Watchtower. Here the CBF and PLF fault zone intersect each other.

Stop 1.4:

Playa Macenas - Punta del Peñon: The intersection of the Carboneras and Palomares fault zones.

(1:25.000 Map Castillo de Macenas, IGN Series)

From the watchtower there are impressive views

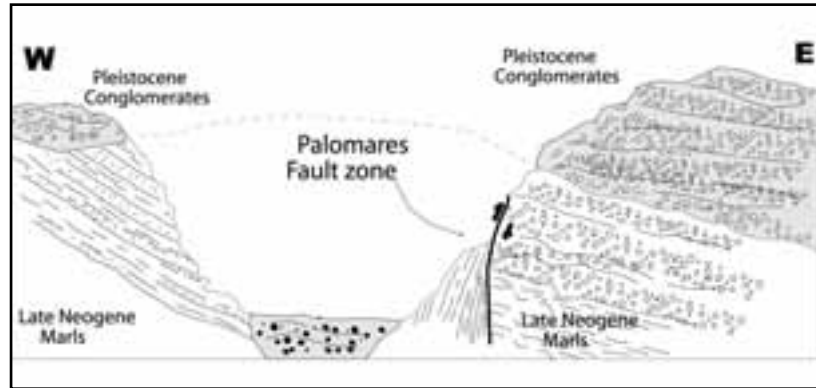


Figure 1.4 - Geological cross-section of the Palomares Fault adjacent to the town of Palomares.

down the coast illustrating the intersection of two large fault zones at the starting point (inflexion) of the EBSZ southern terminal splay. Looking to the south we can observe the geology south of the CBF, with the Cabo de Gata Volcanics overlain by Late Neogene limestones. The view to the north is along the line of the PLF, developed on the black Nevado-Filabride schists of Sierra de La Cabrera and brecciated Triassic meta-carbonates (dolomites) and, occasionally, Oligocene carbonates. Just in front of the watchtower flakes of these materials come along with Langhian intrusive and volcanic rocks, giving a complex fault braiding geometry. In most of the cases these fault flakes present well-preserved slickenslided surfaces (Fig. 1.3), with striations indicating prevalent left-lateral fault displacements striking from N40-60 (CBF) to N10-30 (PLF). Actually, the entire zone of Punta del Peñon is a complex intersection fault zone partially exhumed by littoral processes. In the far distance, looking to the north, you can see the Sierra de La Almagrera. This chain is a block offset from the Sierra de La Cabrera along the PLF for more than 14 km. Several authors consider the accumulated offset of this fault to be from 20 to 14 km (Weijmars, 1987; Coppier et al., 1990), most of which assembled during the last 7 Ma, giving a horizontal slip-rate of 2 to 3,2 mm/yr. In contrast, vertical slip rates are very low, in the range of 0.05-0.04 mm/yr (Goy et al., 1993).

Other features related to the most recent activity of this tectonic structure can be observed while walking down along the coastal track. Sharply-dipping rounded to sub-rounded conglomerates patching the fault zone can be observed adjacent to the watchtower (Fig. 1.3). These conglomerates contain well-rounded large-sized clasts that, in absence of a close rambla mouth, have to be explained as a coastal “colluvial

wedge” reworked by continuous wave action. Whatever the case, large and small clasts are commonly sliced following CBF trends and indicate left-lateral shear. Also, the multiphase OIS 5 (Tyrrhenian) beach deposits are noticeable; these have recently developed a terraced surface, elevated at +6m above the sea level (Fig. 1.3). The Upper Pleistocene beach sequences pass up to weakly-cemented aeolian sands, which at the top display intense burrowing and bioturbation (root casts), occasionally strongly cemented. This fact suggests the development of an ancient soil profile which preceded the younger debris-slope deposits, assumed to be of generic Würm age by some authors (Mather et al., 2001). In fact, the whole Quaternary sequence records the coastline evolution during the Late Pleistocene-Holocene and its uplift (Fig. 1.4). On a regional scale, OIS 5 deposits have vertically displaced a maximum of 5 m north and south of the CBF (Goy and Zazo, 1986; Bell et al., 1997). GPR surveys carried out at Playa Macenas also revealed apparent vertical offsets along the Polopos Fault (CBF) system (Reicherter and Reiss, 2001).

Transfer to Stop 1.5: Return to the main coastal road (AL-118) and turn right towards Mojacar. Continue along the coast until you get to Garrucha. There follow the signs to AL-1065 {near? along? at?} by the city by-pass (head towards Aguilas-Murcia). Leaving Garrucha, en route you can observe the linear ridge, 20-15 m high, on which this village is situated. Pleistocene pre-Tyrrhenian beach deposits raised along the PLF trace constitute the top of the ridge. Continue driving until Palomares, and then take the detour to AL-160. At the first roundabout avoid the main roads and take the road that runs along the Garage wall. After c. 400 m you will reach a trenched road. Continue uphill, at the top a little rambla valley opens to the right. This is a little creek that follows the PLF fault line. Coaches will have to continue ahead to get out of the road-trench (c. 100 m). Walk down the valley along its left margin (that's important!).

After descending the first two artificial banks of the rambla floor you are in front of the first outcrop of the Palomares Fault described in the scientific literature (Bousquet and Phillip, 1976).

Stop. 1.5:

The Palomares Fault west of the village of Palomares.

(1:25.000 Map Burjúlú, IGN Series)

At this point we can explore this pristine outcrop of the PLF. The fault zone pushes the Pliocene yellow marls (west) against Pleistocene conglomerates (east) following a N10 orientation along the left margin of the creek. At this margin a relatively narrow, and indurated fault gouge developed in the marls, forming a triangular-faceted little shoulder patching the superb fault-mirror that charmed the French geologists. This slickensided plane is curved, since in the basal Pleistocene conglomerates dip 81° WNW, whilst in the basal indurated marls dip 75°ESE (Fig. 1.4). Some isolated outcrops along the creek seem to suggest a wide flower positive structure, presently eroded by the creek-valley. Kinematic features preserved in the fault plane are subhorizontal striations, 2-10° pitch to the south, indicating left-lateral offset. The pitch

cases indicate that the western block of the fault was uplifted relatively to the eastern block (the footwall), facilitating the accommodation of new conglomerate sequences of the Almanzora River during the Middle Pleistocene (Goy and Zazo, 1986). Coming back to the trenched road, many brittle deformations of the youngest conglomerates can be observed along the western side. These mainly related to minor reverse and subsidiary normal faulting within the middle Pleistocene conglomerates. In spite of clear evidence of palaeo- and present-day seismicity in the PLF, it is traditionally associated with the X MSK event that destroyed the city of Vera in 1518 AD.

Transfer to Stop 1.6: Go back along the route to coastal road AL-1065 and turn left (towards Aguilas-Murcia). Cross the bridge over the Almanzora River,

and drive all the way through Villaricos. 11 km on, after the Pozo del Esparto sign, take the first road to the right (towards the coast). Follow this road and park next to the Guardia Civil House (now in ruins). Looking to the north there is a little rocky promontory. This is stop 1.6, follow the pathway (ca 200m) to reach it.



Figure 1.5 - Panoramic view of the sequence of middle and Upper Pleistocene marine units outcropping at Pozo del Esparto.

of striation increase from 2 to 10° from the basal marls to the upper conglomerates, suggesting that vertical dislocation may have been reached during the Quaternary evolution of the fault. In fact, only the first basal conglomerate unit (4-5 m thick) is affected by the fault; above that the rest of the conglomerates (6-8m thick) seem to be adapted to the PLF trace, yet otherwise undisturbed. Apparent fault throw at both sides of the creek is about 9-11m, which matches the overall topography of the zone. Both

Stop 1.6:

Pozo del Esparto: OIS 5 Blind faults and reverse flexures of the PLF System.

(1:25.000 Map Pozo del Esparto, IGN Series)

A first sight of this stop from the Guardia Civil ancient house will give us a panoramic view of the sequence, and mainly of the geomorphological disposition of the analysed units (Fig. 1.5), which will be interpreted from a tectonic point of view. This coastal sector is located within the westernmost tectonic domain of

the Aguilas Arc, which is affected mainly by N10-20 faults, that is, the PLF system. The work of these faults during the Early-Middle Pleistocene triggered the opening of the so-called Los Arejos Corridor (Bardají, 1999), the coastal southern termination of which is discussed at this stop, while the northern termination will be visited during next Stop 1.7. In this coastal sector one of these faults appears to be a blind reverse fault, that behaves on the surface like a flexure axis, affecting OIS 7 and OIS 5 marine units. The sequence outcropping at Pozo del Esparto consists of six Pleistocene marine units, with different geomorphological and spatial dispositions, developed over the Upper Pliocene- Lower Pleistocene yellow calcarenites. A first conglomerate marine unit presents shoreface sublittoral facies; this is separated from the second conglomeratic unit (foreshore facies) by erosional red terrestrial deposits. These units are clearly affected by the aforementioned reverse N10-20 fault, which also conditioned the deposition of the younger units. These four younger units develop in a slightly staircase manner, determined by the coeval working of the fault as a flexure axis. The U-series dating on *Strombus bubonius* found in the first three units (Goy et al., 1993) allowed us to correlate them with OIS 7, ISS 5e and ISS 5c, and the most recent one (containing *Arca* sp.) has been ascribed to the Holocene. The height at which these units outcrop at present are +7m, +4m, +3m and +0.5m, so by following the same assumptions stated in Stop 1.1 (that is, the position of sea level during ISS 5e at +2m a.m.s.l.), this sector has undergone a tectonic uplift of 0.015 mm/yr since the last Interglacial (ISS 5e).

DAY 2

The Murcia Region: The Alhama de Murcia-Lorca Strike-slip fault zone.

J.J. Martínez-Díaz, P.G. Silva and E. Masana

During this second day we will examine the geology and geomorphology of the Lorca - Alhama de Murcia Fault Zone (LAF). This is one of the best developed strike-slip faults of SE Spain, and displays thematic outcrops of: the crustal structure of SE Spain, surface faulting, tectonic geomorphology, and paleoseismicity. The LAF first described by Bousquet and Montenat (1974) defines the central segment of the EBSZ as over more than 100 km. Several studies have since led to its division into three main fault segments, separated by major fault bending, branching and the development of contractional duplexes (Silva et al., 1992; Silva 1996). In these segment

boundaries the strongest seismic events recorded during the instrumental period nucleate, leading to its identification with individual earthquakes: for example, the 1977 4.2 mb Lorca event (Mezcua et al., 1984; Martínez Díaz, 1999).

Transfer to Stop 2.1: Leaving Aguilas, take Motorway N-332 and continue on until Lorca. Reaching the city of Lorca, follow the signs towards the Autovía del Mediterráneo (N-340). Go along this motorway to the south (towards Almería) and take the Hospital Rafael Méndez exit. At the end of the deceleration lane turn right onto the road, and follow down it. Park the vehicle and walk down the road until you get to the rambla crossing.

Stop 2.1:

Rambla de La Torrecilla. The Alhama de Murcia-Lorca fault gouge.

(1:25.000 Map Campillo, IGN Series)

On both banks of the rambla, under the gaze of an ancient Arab watchtower, one of the most impressive fault gauges of the Betic Cordillera can be observed in detail. The paleozoic schists of the Alpujárride complex were transformed by the shear produced along the LAF in a dark-coloured fault gouge (Fig. 2.1) The fault zone is oriented N 40°-45°E and separates the metamorphic materials of the Las Estancias Range from the Quaternary alluvial deposits of the Guadalentín Depression. The shear zone dips 60-70° SE and is more than 5 m in width. The fault gouge, widely studied by English geologists in order to compare its structure with laboratory-induced fault gouges (Rutter et al., 1986), shows many kinematic traits indicating an oblique reverse-strike-slip

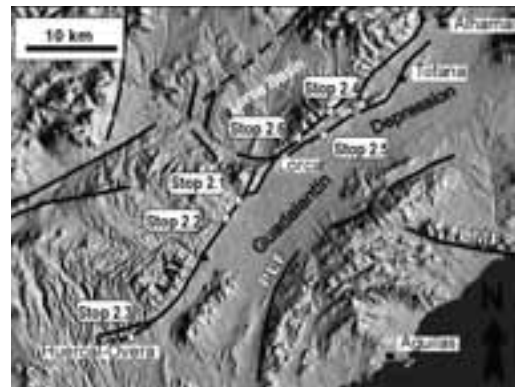


Figure 2.1 - Digital elevation model showing the location of the Day 2 stops, within the framework of the Central Segment of the Eastern Betic Shear zone.

movement. The fault rock, formed in phyllosilicate-bearing rocks over a wide range of environmental conditions within the Earth's crust, are characterised by similar structural and microstructural features. The most striking of these are: **P** foliation, defined by the preferred alignment of phyllosilicates along a plane oblique to the direction of the shear and small-scale shear zones either parallel to the shear direction (**Y** shears) or oblique to the direction of shear but with the opposite sense of obliquity compared to the **P** foliation (Riedel shears, **R₁**). The minor shear zones have the same displacement direction as the host shear zone (Rutter et al., 1986).

The clay-rich fault gouge exhibits an evident **P** foliation, demonstrated by the orientation of clays and cataclastic mica fragments, at 150° to 90° to the fault walls, by **R₁** shears spaced a few centimetres apart, and **Y** shears. Orientation data from this outcrop, show constant angular relations between **P**, **Y**, and **R₁** surfaces, and the slip vector. The intensity of development of the **P** foliation and **R₁** shears is generally uniform throughout the whole volume of the fault gouge; thus the gouge can be said to have flowed fairly homogeneously within each gouge sliver. The tendency of the deformation to be uniformly spread throughout the gouge may indicate that strain hardening processes were operative (Rutter et al., 1986).

Transfer to Stop 2.2: Go back the way you came to get back on to the Motorway (N-340) and head towards Almería. Take the first exit (on the right) signed "Poligono Industrial de Lorca". when you reach the roundabout turn right along the main road heading towards the ITV Plant. Continue until the end of this road and then turn right towards the CANAL Factory. The road ends in a wide parking lot. Head towards the NE corner of the parking lot and take the large truck-road for the quarries (suitable for coaches). Follow this road and park the vehicle on the shoulder just when you are entering into the mountain front. To the right there is a spur ridge. Climb up to the ridge top.

Stop 2.2:

Rambla del Borruezo. Left-lateral drainage offsets and tectonic geomorphology of the fault zone. (1:25.000 Map Campillo, IGN Series)

This stop is situated about 3 km southwest of the previous one. It is also in the southern segment of the LAF and illustrates the tectonic geomorphology of a typical crustal-scale strike-slip fault zone (Fig.2.1). We have to walk up to the crest top to the north. In

the far distance, looking to the north, you can see the Castle of Lorca and the nearby little watchtower of "La Torrecilla" (previous stop). These landmarks outline the mountain front that developed along this fault segment, as well as the more discrete set of spur (pressure) ridges adjacent to it. In fact we are standing on a little spur ridge of the fault some 80-100 m wide. Looking now to the nearby rambla outcrop, we can see the internal structure of these spurs. High-angle reverse faulting overthrusts and pushed up the red Triassic beds and Alpujarrian phyllites over the Plio-Quaternary conglomerates (marginal fan systems). Along the adjacent valley, to the left, runs the main fault zone, about 500 m wide in this sector. The fault zone is made up of a set of fault gouges of Alpujarriide (schists and phyllites) and Malaguide (red-wine beds) among which relatively undeformed flakes of Tortonian conglomerates, Messinian(?) marls, and



Figure 2.2 - Detailed view of the Lorca-Alhama de Murcia (LAF) fault gouge, South Bank of La Torrecilla Rambla

Precambrian/Cambrian schists are sandwiched. Now we have to retrace our steps back to the path along the crest of the spur ridge until its southern termination over the Rambla del Borruezo. Looking to the

south, towards the industrial zone's water tower, four different ridge-hills spur between the present rambla valley (to the west) and the Guadalentín Depression (to the east). The rambla valley runs along the main fault zone, obvious from this point by the multicoloured-banded landscape.

The aforementioned hills correspond to individual fan bodies made up of proximal conglomeratic lobes separated by finer distal sands and variegated clays. This present assemblage of sedimentary bodies is a primary consequence of the successive overlapping of fan lobes to the NE for about 1600 m, which indicates the dominant left lateral behaviour of the LAF in this segment (Fig.2.3). Looking to the present rambla valley we can now observe the most recent impact of left-lateral kinematics on drainage development. The present rambla traces a prominent bayonet more than 250 m in length. Today it is possible to observe the actual offset channel (trenched) and the former beheaded channel (untrenched). Surveys of this zone indicate that channel offsets were a main characteristic of this particular sector of the LAF prior to the southern segment termination at the Lorca Contractual Duplex (LCD). The more recent left-lateral displacement recorded by channel offsets range between ca. 50 to ca. 25 m, from south to north, suggesting a progressive buffering of displacements towards the LCD, where major earthquake nucleation takes place. Instrumental seismic records seem to indicate that aseismic creep operates in this fault segment accumulating tectonic stress over the LCD (a segment boundary) where major earthquakes are prone to occur (Silva, 1996).

Transfer to Stop 2.3: Go back along the route and take the Motorway (N-340) again towards Almería. Continue until the exit marked "Huercal-Overa and Sta. Maria de Nieva", which is about 30 km south of Lorca. At the end of the deceleration lane turn right towards Sta. Maria de

Nieva. After ca. 500m take the first road to the right immediately beyond the warehouse of Transportes CABRERA. Continue down the road (suitable for coaches) until the first house. Here park the vehicle and take the right path uphill until the outcrop (just over the house).

Stop 2.3:
Rambla del Ruchete

At this point we can see the western edge of the LAF along the southern border of the Las Estancias range and separates this sierra from the Huercal-Overa Basin. In this area the LAF changes to a more E-W orientation forming a horse-tail pattern. In this area this fault interacts with previous E-W faults that generated the half grabens in the eastern part of the Huercal-Overa Basin. The principal fault displacement is distributed along several parallel displacement faults that deforms Quaternary alluvial fan deposits coming from the north. In this outcrop we can observe the fault structure on the walls of several

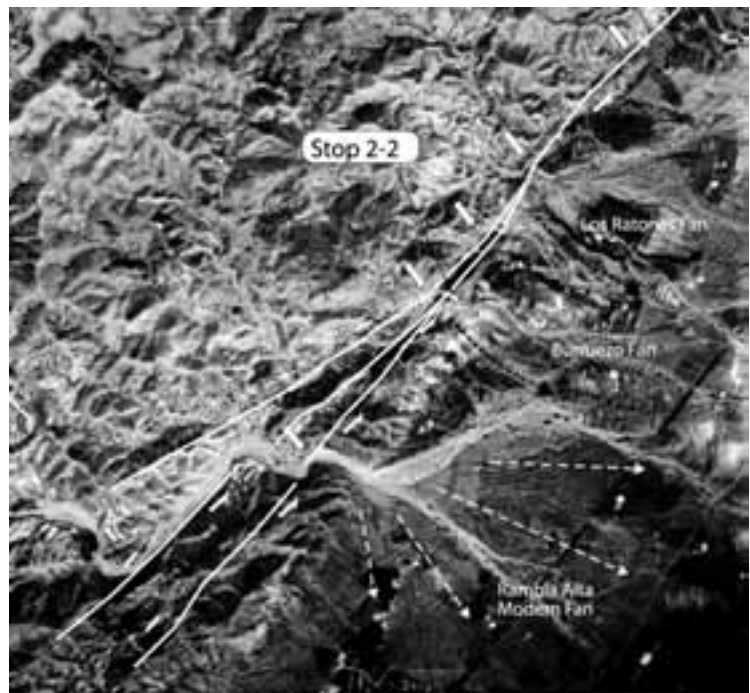


Figure 2.3 - Aerial Photo (American Flight 1956) showing the structural arrangement of the left lateral displacement zone of the LAF between Rambla Alta and La Torrecilla. Arrows indicate major drainage offsets. Black dotted arrows indicate ancient beheaded fan channel. 1 to 4 indicate ancient individual fan lobes displaced along the fault zone. Aprox. Scale 1:33.000.

paleoseismological trenches made by the Barcelona and Complutense Universities. Spectacular folds and faults affecting alluvial gravels show the reverse component of the movement (Fig. 2.4). The paleoseismic activity of this sector of the fault is now under study and the conclusions are still incomplete. A preliminary analysis of the walls of the trenches shows high-angle and low-angle reverse faults that control the Ruchete hills to the north. These faults produced impressive drag folds in the quaternary alluvial gravels. Preliminary Thermo-Luminiscense datings give the most recent silt layers ages from 7,000 to 2,000 years BP. Preliminary interpretation does not allow us to calculate a reliable recurrence interval.

Transfer to Stop 2.4: Go back along the route to the Motorway (N-340) and head for Murcia. When crossing the Tunnel of Lorca we will also be crossing the sector of the LAF Fault-zone in which the strong earthquakes nucleate. On the opposite end of the tunnel, after the bridge over the Guadalentín River, we will be going into the Central segment of the LAF. This is both the most active and most complex segment of the fault, and the sole objective of the second half of today's field trip. Now continue along the Motorway and take the exit marked "La Hoya". Drive downslope and turn right at the ancient main road, N-340b. Take the first road to the right (about 200m away from the intersection) and drive up slope. This small road is suitable for coaches only until the little bridge over the Transvase Tajo-Segura Channel, but minibuses and vans can continue up the hill until the

ancient Chapel of Our Lady Virgen de la Salud. Here, park the vehicle and climb up the little hill located at the eastern end of the parking lot.

Stop. 2.4:

Rambla de La Virgen de la Salud: A view-point for the Central segment of the LAF.

(1:25.000 Map Lorca, IGN Series)

From this standpoint, looking to the east we can observe in the far distance the forms of Sierra Carrascoy (north) and Almenara (south) located at the eastern margin of the Guadalentín Depression. The intervening gap corresponds to the ancient outlet of the Guadalentín fluvial system to the Mediterranean (Campo de Cartagena – Mar Menor Basin), formerly redirected towards the north by tectonics (Fig. 2.1). From this viewpoint we also have an excellent overview of almost the entire central segment of the LAF, which branches into two main faults. La Tercia Fault (LTF), to the NW, gives place to the main faulted mountain front with a broad N45-50 orientation. The Guadalentín Fault (GDF), to the SE, affects the Lower-Middle Quaternary fan systems. This last fault has a main N60-70 orientation, favouring the compressive tectonics, and giving rise to intervening pressure ridges between the range front and the main tectonic depression.

To our back (in the west), we can observe the immediate relief of Sierra de La Tercia (Fig. 2.1). This

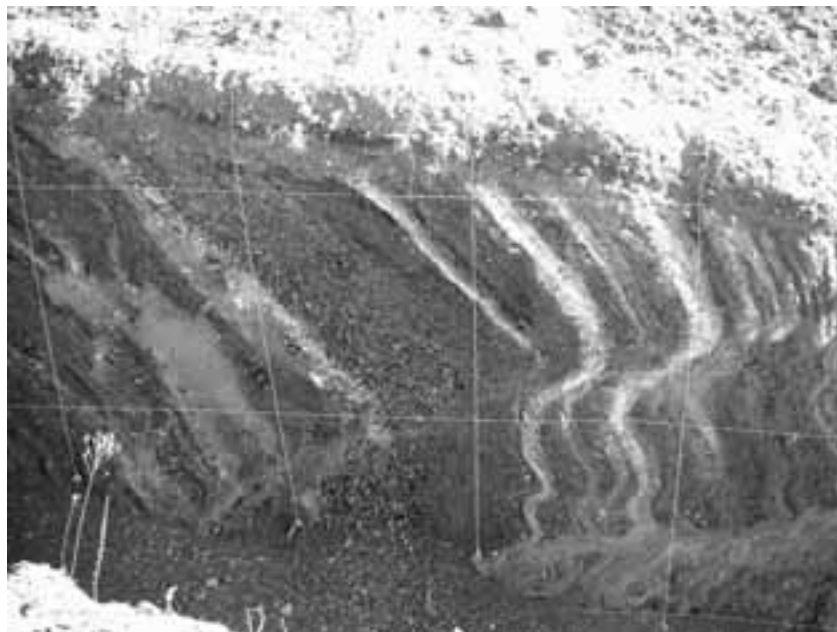


Figure 2.4 - Alluvial fan gravels affected by the reverse activity of the LAF in the TR2-Ruchete trench.

is a large-scale asymmetric antiform developed on metamorphic Alpujáride Complex materials (schists and mica-schists), topped by Tortonian carbonates, and limited by the LTF, on which we are standing. This fold was created by the reverse activity of the LTF from the Tortonian to the Quaternary and it presents a complex structure of blocks bounded by normal faults generated during uplift (Martínez-Díaz, 2002). Differences in the altitude between the Tortonian carbonates topping the relief and those involved in the fault zone led to estimating an accumulated fault throw of about 500 m and mean uplift rates ranging between 0.08 to 0.09 m/ka for the last 6 Ma. The TLF is a high-angle reverse fault dipping to the NW in which different flakes and blocks of Betic metamorphic rocks, Messinian marls and Tortonian carbonates and conglomerates are involved.

To the south (on your right) we can observe the adjacent outcrop of the Rambla de La Salud (Fig. 2.5). This illustrates both the structure of the fault zone and the progressive unconformity (proximal offlap progradation) outlined [?] by the Pliocene to Middle Quaternary alluvial systems in response to fault activity (Silva et al., 1992a). Note that immediately downstream from the marly fault gouge, the conglomerates are subvertical and have a colluvial character including blocks of 1.7-1.9 m diameter. Syndepositional reverse and normal growth-faults (but also gravitational sliding) affect these materials. The top of this colluvial unit is beheaded by a major angular unconformity. The first unconformable unit (1 in Fig. 2.5) is mainly comprised of medium-to-large-sized “tablets” of Tortonian carbonates (the yellow-coloured unit), attesting to the incorporation of the La Tercia top mountain to the headwaters of the alluvial fan systems, and the eventual organisation of the present landscape. Typical alluvial fan deposits of a more “fluvial” (channelled) nature constitute the rest of the alluvial sequence (up to 12 m thick), deposited between the two branches of this fault segment. Looking again to the east, we can observe firsthand the geomorphology linked to the second branch of the segment (GDF). This features a set of pressure ridges and/or reverse fault scarps preferentially developed in Messinian gypsums, but also affecting the aforementioned middle Pleistocene alluvial fan sequence, which is overthrust. The fault throw here ranges between 10-15m. The present rambla valleys are incised on both the alluvial sequence and pressure ridges. These form the present mountain front location, marking the apex of the most recent

late Pleistocene to Holocene fan systems of the actual Guadalentín Depression. A more precise description of the GDF will be available at the next stop.

Transfer to Stop 2.5: Retrace your steps to the road and come back to the old main road N-334b. Turn right (south) and drive through the town of La Hoya. Just before you leave this town take a little road that runs parallel to the road along its right side. At the end of the row of houses that you have on the right, turn right and follow the road traced along the rambla floor. If in coach and/or minibus you have to park just after the passage under the Motorway and continue on foot. Climb up until the Transvase Channel, cross the bridge, and take the little trail to the right that comes back down to the rambla floor. After ca. 300m you have on the right a prominent pressure ridge along the GDF trace and, to the left, an ancient site for paleoseismic analyses trenched in recent rambla deposits. This is stop 2.5.

Stop 2.5:

Rambla Colmenar

(1:25.000 Map Lorca, IGN Series)

This site is situated on the right bank of the Rambla Colmenar creek, where this crosses the GDF after a sharp right bend of the channel (Fig. 2.6). Based on the geomorphologic analysis the alluvial terrace sediments covering this area appear to be the most recent sediments in contact with the fault and thus this is a good site for detecting the most recent deformation events along the fault. Radiocarbon dating have come up with Holocene age for these sediments (Martínez-Díaz et al, 2001).

The morphology of the area is made up of a small hill (microtopography in Fig. 2.6) bounded to the north by a gully draining towards southwest. A small outcrop of Miocene substratum is located on the southern part of the hill. Fan deposits (unit 5 in Fig 2.5) are in sharp contact with this substratum to the north, and are overlaid by a northwest dipping (tilted by the fault activity) calcrete soil at the northern part of the hill. The top of the fan with a thick calcrete outcrops in the deepest part of the gully. Younger Holocene alluvial terraces unconformably overlay the described units. The trench excavated on the natural bank of the Colmenar creek is nearly orthogonal to the fault and allows us to observe in detail the GDF structure and its recurrent paleoseismic activity.

This one-wall trench is 15 m long and up to 5 m high

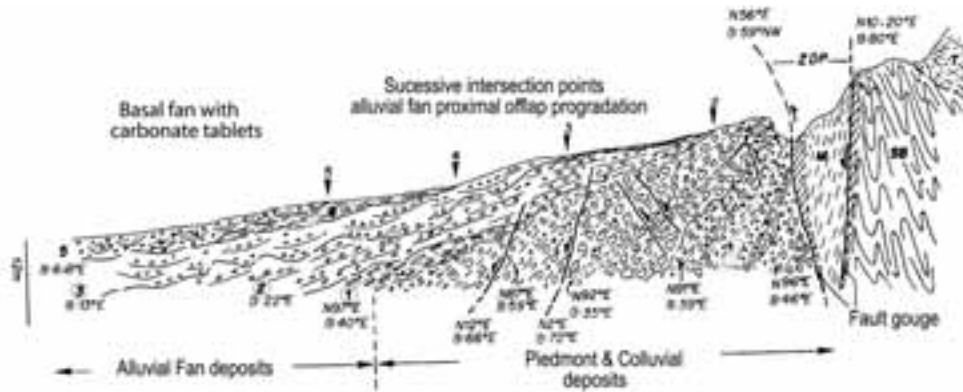


Figure 2.5 - Geological cross-section along the southern margin of Rambla de la Salud, showing the structure of the LTF fault and the progressive unconformity assemblage of the different colluvial to alluvial fan sequences (1, 2, 3, 4, etc.). Numbered arrows indicate the former positions of the related intersection points of alluvial fan bodies. ZDP: Principal Displacement Zone of the LTF. SB: Betic substratum; T: Tortonian; M: Messinian.

(Fig. 2.6). It shows a deformed area at the lowest part of the wall, produced by several SE low dipping reverse faults which converge at the southeastern-lowermost part of the trench. The rest of the faults show reverse slip components at the trench section. The only difference is the lower dip of the fault planes.

The stratigraphic units are shown in Figure 2.6 Most of the faults are sealed by units C, D and E. Only one fault, the flat southeastern-most one (Fault 2), cuts slightly, but clearly, through unit D. Geometrical and sedimentary features observed in this trench can be used to identify paleoseismic activity. Internal deformation and tilting of units A to E, as well as abrupt sedimentary environment change observed in unit C, have all been used to infer several coseismic events (Martinez-Díaz et al., 2001; Masana et al., 2004). The red sediments of unit C present very different characteristics compared to the rest of the stratigraphic sequence observed in this area. The only possible source for the yellow clays and silts of the matrix of this unit are the Neogene marls that crop out only along the hanging wall of the southeastern fault strand, that is, downstream. The source area for the rest of the units, which are metamorphic and calcareous rocks from the La Tercia range, is located to the NW. The fine-grained sediments in unit C indicate a lower energy depositional environment

associated with sediments formed under damming conditions produced by a sudden uplift of the hanging wall of the southeastern fault and the formation of an unstable scarp along the fault. This is traced to the older of the two paleoearthquakes identified in this trench. The younger event took place between the deposition of units D and E, i.e. between 2130 and 830 yr BC. The older event must have taken place just before the deposition of unit C and long after the formation of unit B (a soil), which is the youngest deformed layer before unit C, i.e. between 125 ka and 16670 yr BC (but probably a short time before the latter). The correlation of this data with the trenches analyzed in the El Saltador fan show that the southern branch of the LAF (GDF) is seismogenic and that it has generated a minimum of two earthquakes in the last 18 ka (approx.), the last one being very recent and possibly historical (around 1460 yr AD). The previous event took place shortly before 16.4 ka. The maximum magnitude obtained from the rupture area and from the slip per event measured at the trenches is $M_w=7.0\pm 0.1$, which exceeds the largest earthquake recorded in the seismic catalog. The fault shows a left lateral and reverse sense of slip. The vertical slip-rate obtained is 0.10-0.20 mm/yr and the strike slip-rate is 0.15-0.32 mm/yr (Masana et al., in press).

Transfer to Stop 2.6: Retrace your steps back to the Tajo-Segura Channel and take the service road towards the west. Park the vehicles close to the third bridge over the channel, cross it and continue on foot. Walking 1 km you will come to a junction of both branches of the Alhama Fault zone.

Stop 2.6:
Carraclaca
 (1:25.000 Map Lorca, IGN Series)

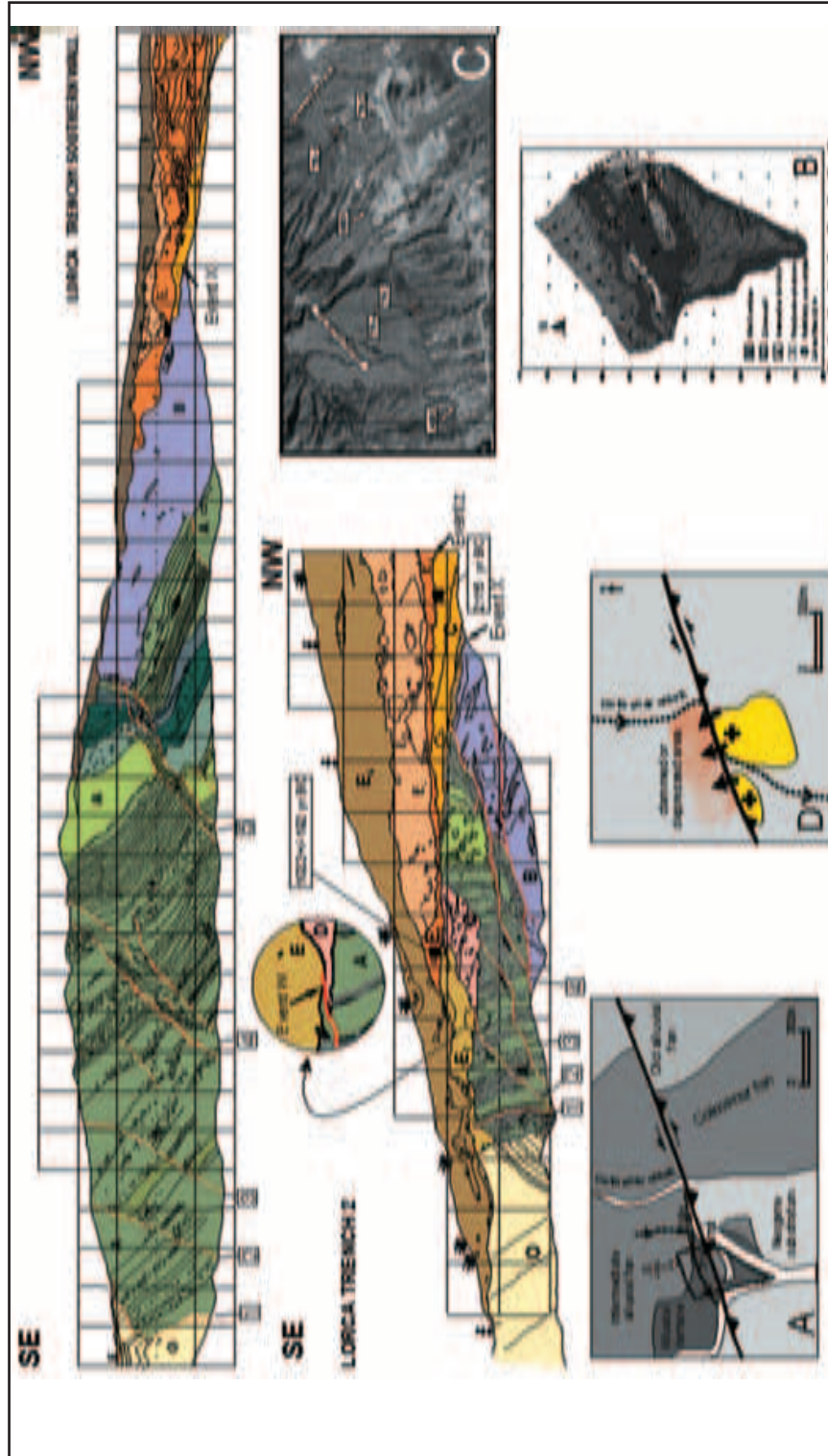


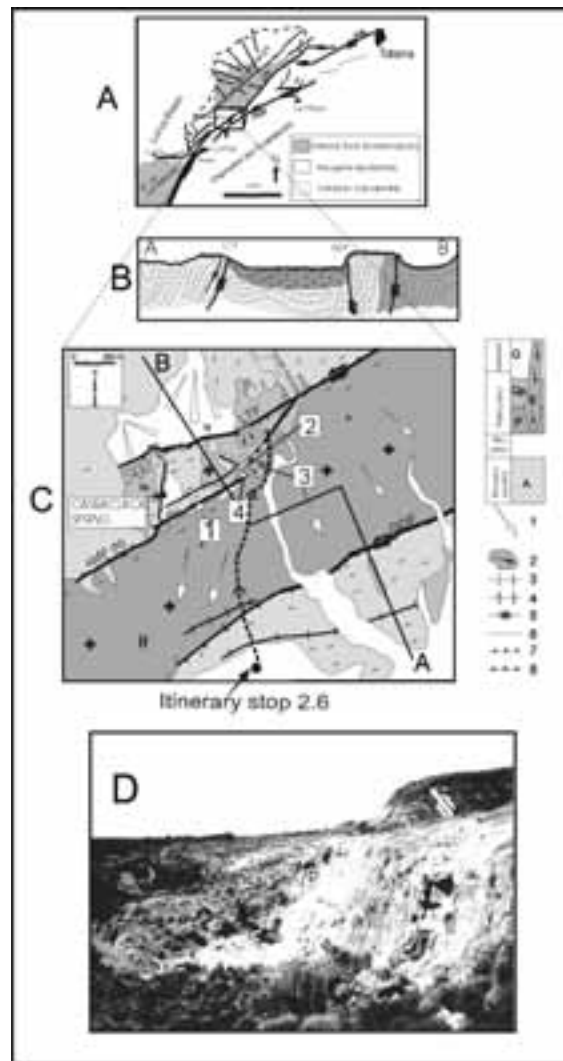
Figure 2.6 - Logs of the southwestern wall and part of the northeastern wall of trenches 1 and 2. The different colors and letters distinguish the different sedimentary units. The several reverse oblique-slip faults affecting quaternary units are numbered. Arrows indicate the position of the different event horizons. The absolute age of unit E₃ obtained using the radiocarbon AMS method is also shown. -A: Sketch of the geomorphic units in El Colmenar creek area, in the surroundings of trenches 1 and 2. B: Microtopographic map of the right bank of El Colmenar creek where it crosses the southern Alhama de Murcia fault. Location of trench 1 and preliminary sampling location are shown. The position of the microtopographic map (A) is also marked. This sketch also indicates the control of the Alhama de Murcia fault trace on the alluvial channels. The trenches were located where the most recent alluvial terrace deposits are in contact with (need a subject here). C: Aerial view of the fault with the location of the trenches excavated. D: Interpretative sketch of the event X. Sedimentary units O: Neogene substratum (marls and gypsum). A and B: alluvial fan deposits, coming from NW, with calcarete levels. C: Fine red sand with clay-rich matrix. The source of this unit is the erosion of unit O. D and E: alluvial deposits from younger terraces of Colmenar creek. F: Current soil.

From the bridge the path goes along upper Miocene marls and gypsums that are folded and highly dipping due to the activity of the GDF. Then cross the fault that deforms Quaternary limes and gravels; for about 600 m you'll be walking over the depressed area produced by the antithetic reverse movements of both branches: the northern branch dipping NW, and the southern branch dipping SE. After a short walk you'll arrive at the Carraclaca site.

The Carraclaca site coincides with the ancient Carraclaca Roman hot spring, active until the last century. Currently, the low water flow coming out makes it impossible to use their thermal and medicinal waters. Carraclaca spring is located in an area where the TLF has a left-stepping structure with two main faults connected by N-S and NE-SW faults. This produces a relatively complex tectonic structure affecting deposits from Upper Miocene to Quaternary. The two main overstepped reverse faults have opposite dip direction giving rise to block uplifting that produces a pop-up structure (Fig. 2.7) bounded by two monocline drag folds, which affect cemented Quaternary alluvial fan deposits. The pop-up is asymmetric due to the higher amplitude of the southern monocline fold controlled by the main fault plane of the AMF. Taking into account the sinistral strike-slip component of the reverse oblique-slip fault movement in this area (Armijo, 1977), the structure acts as a dilatational overstep (Martínez-Díaz y Hernández Enríe 2001) (Fig. 4). So, it is possible to observe fault planes with reverse and opening movements into the pop-up, affecting Pleistocene alluvial fan deposits. The reverse movement is more frequent along minor faults parallel to the main fault zone (N 55-60 E). Faults oriented northward (evidence on the southern flank) have a mainly opening movement with several opening cycles that may be interpreted as sudden-fold uplift events linked to reverse movements along the TLF (paleoearthquakes?).

The structural complexity of the area make the existence of many rising water points possible in different topographic positions. This produces a 1 km² area in which it is possible to observe travertine layers overlapping Upper Miocene marls and conglomerates, and Quaternary alluvial fan deposits. Following the morphological classification of travertine deposits proposed by Hancock et al (1999), we

Figure 2.7 - A: Structural scheme of the Lorca-Totana segment of the Alhama de Murcia Fault Zone: LTF: Lorca-Totana Fault. B: Geological cross-section showing the pop-up structure in the LTF in which Carraclaca travertines appear. C: Geological map of the Carraclaca spring area. This spring occurs where two fault planes of LTF form an overstep structure. In some places travertines overlap the main faults and they are deformed in different grades. D: view from the east of the outcrop A: Messinian marls; P, Qp and Q: alluvial fan deposits (gravel and silt) coming from the La Tercia range. E: Travertine deposits, the arrows show flow direction. 1: Direction of alluvial fan transport. 2: Travertine patches and flow trend. 3 and 4: Anticline and syncline axis. 5: Strike-slip fault. 6: Reverse fault. 7: Normal fault. D-D': cross-section shown in Fig. 11a. Numbers 1 to 4 point out the position of the dated travertine samples.



can distinguish four different morphologies in this area, depending on their relative position to the main fault zone and local features. The type of precipitation deposits depends on the geometry of the structure controlling the water source. If it flows out through a sub-vertical fracture, water spill produces calcite precipitation covering the topography, and then dike filling of the opened fracture.

The reverse component of movement of the fault produced a 15 m amplitude monocline fold at the Carraclaca site, growing from late Pleistocene to the present. U-Th absolute ages for deformed and undeformed travertines give a vertical slip rate of 0.08 mm/yr. Using the slip per event affecting alluvial deposits on the southern branch of the LAF fault Martínez-Díaz et al. (2001) estimate a recurrence time of less than 5000 yrs for the TLF.

DAY 3

The Alicante region: the Bajo Segura and Crevillente faults.

P. Alfaro and A. Estévez

On this day we examine the Northern onshore Terminal Splay of the Eastern Betic Shear Zone. This transpressive area, where the Bajo Segura basin lies, is one of the most seismically active areas of the Iberian Peninsula.

In contrast to the generally low-magnitude seismic activity along the whole Betic Cordillera, several destructive earthquakes (Io/VIII) have occurred in the past in the Bajo Segura basin. The 1829 earthquake (Io = X MSK; Ms = 6.3-6.9) destroyed the town of Torrevieja and caused serious damage and loss of life in the area. According to historical reports there were 389 deaths, a total of 2965 houses totally destroyed and 2396 houses partially damaged. In addition, other historic earthquakes, with a lower intensity at the epicentre (VII-VIII), have been experienced in the southern part of the basin: at Guardamar del Segura (1523), Rojas (1746), and Torrevieja (1802, 1828, 1837, 1867 and 1909). During the twentieth century the Jacarilla-Benejúzar earthquake of 1919 (mb = 5.2) and its aftershocks stand out.

This seismic activity is mainly linked to the Crevillente and Bajo Segura faults, running ENE-WSW and E-W respectively, and to several NW-SE right-lateral faults (Guardamar del Segura, Torrevieja and San Miguel de Salinas). In contrast to what occurs in the central sector of the EBSZ, these faults in the northern sector

of the shear zone do not rupture at the surface. Their main superficial expression is the folding of the most recent rocks dating from the Late Miocene, Pliocene and Quaternary (Goy and Zazo, 1989; Montecat, 1977; Alfaro et al., 2002a).

Folding is not synchronous over the whole basin, as can be deduced from an analysis of the progressive unconformities developed along the fold limbs. It is deduced that one set of folds started during the Late Miocene, while others started during the Early Pliocene or even during the Quaternary (Alfaro et al., 2002a). As a consequence of this active folding and faulting, positive reliefs have been generated (e.g. El Colmenar, El Altet, Santa Pola, La Marina, Guardamar) as well as relative subsident areas (e.g. El Saladar, Clot de Galvany, El Pinet, Bajo Segura river).

Transfer to Stop 3.1: Take the A-7 Motorway from Murcia towards Alicante. Take the exit for Orihuela and take the CV-920 towards Guardamar del Segura. At the town of Algorfa turn right, onto the CV-935 (towards Torrevieja). After 4.3 km stop at a small piece of open ground next to the entrance to a farm. To the west we can see a panoramic view of the Benejúzar anticline.

Stop 3.1:

Sierra de Benejúzar

(1:25.000 Map Benejúzar, IGN Series)

At this stop the recent deformation produced by the Bajo Segura blind Fault can be observed. This active fault extends onshore from southwest of Orihuela to Guardamar del Segura, in a ENE direction, and continues in an easterly direction towards the Mediterranean Sea (Fig. 3.1).

This reverse fault offsets Triassic carbonate rocks (Alpurrida basement) and folds an Upper Miocene-Quaternary sedimentary cover. In the Benejúzar Sierra, a borehole made for oil exploration cut the basement at a depth of 1550 m. Here seismic profiles indicate that the hangingwall has been uplifted by more than 500 m compared to the footwall (located to the north of the Bajo Segura Fault). The activity of this blind fault develops ENE-WSW asymmetric anticlines, with steep forelimbs in the north and gentle backlimbs in the south (Fig. 3.2). The Benejúzar anticline is one of these folds with a northern limb dipping approximately 50° northwards and a southern limb dipping 20° southwards.

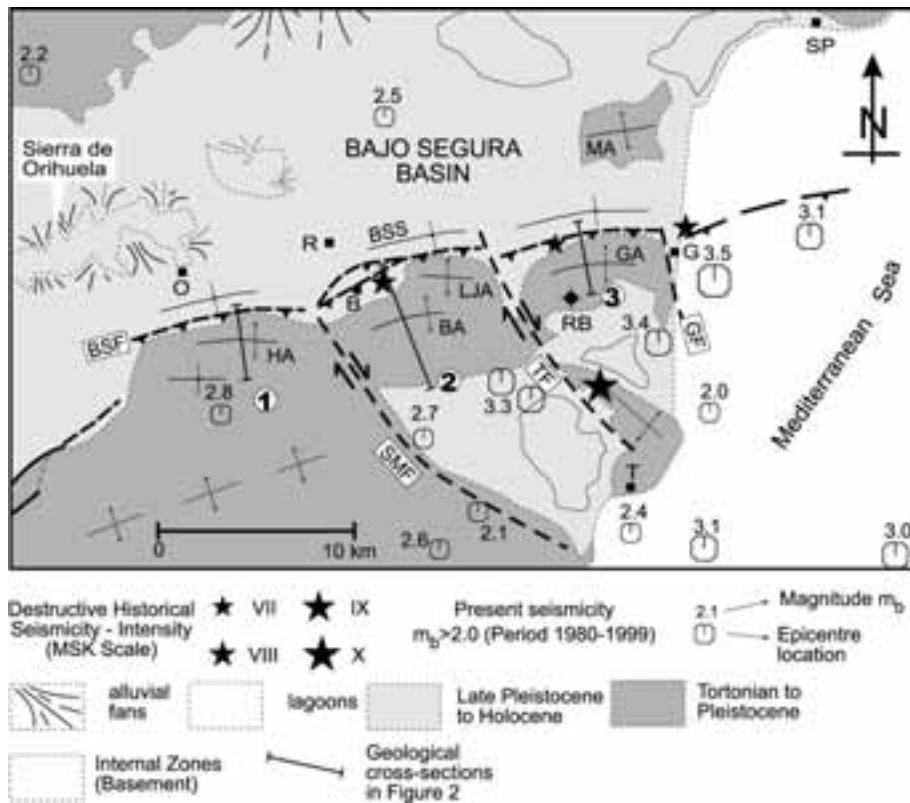


Figure 3.1 - Geological map of the southern Bajo Segura basin. BSF: Bajo Segura Fault, SMF: San Miguel de Salinas Fault, TF: Torrevieja Fault, GF: Guardamar Fault, HA: Hurchillo anticline, BA: Benejúzar anticline, LJA: Lomas de la Juliana anticline, GA: Guardamar anticline, MA: La Marina anticline, BSS: Bajo Segura syncline. Towns: Santa Pola (SP), Guardamar del Segura (G), Torrevieja (T), Rafal (R), Benejúzar (B), Orihuela (O). From Alfaro et al. (2002).

On either side of the Benejúzar anticline, two synclines (areas of relative subsidence) have been formed and filled by syntectonic Plio-Quaternary deposits. The Torrevieja lagoon has formed in the southern subsident area, while in the northern area the Segura river flows from Benejúzar to the sea, running parallel and very close to the northern limb (forelimb) of the anticline. The asymmetric morphology of the fold, the present dip of the Plio-Quaternary deposits, and the location of the Segura river, which flows along the depocentre of the growth syncline (very close to the northern forelimb) suggest that the Bajo Segura Fault dips rather steeply towards the south.

Transfer to Stop 3.2: Go back along the CV-935 towards Algorfa. In Algorfa take the CV-920 heading towards Benejúzar. Go straight ahead across the

roundabout as you approach Benejúzar along the CV-920, and after 300 m. take an asphalted road to your left (just before an industrial warehouse belonging to the company "Ajos Imperio"). Continue along this road in a southerly direction. At 1.3 km the road crosses the Conglomerate Formation.

Stop 3.2 (en route):

The Segura Conglomerates.

(1:25.000 Map Benejúzar, IGN Series).

The analysis of three high-resolution profiles made in the Bajo Segura Basin, indicates how the Pliocene and Quaternary sediments were deformed by the activity of the Bajo Segura Fault. On the basis of the pre-growth and growth strata (syntectonic strata) of these sediments, it is possible to deduce that this fault began its activity during the deposition of the Segura Conglomerate Formation. Therefore, the Segura

Conglomerate Fm, built up by alluvial fan deposits, is the best structural marker for estimating the activity rate of the Bajo Segura Fault, one of the most representative seismogenic structures of the Cordillera. Nevertheless, there is some disagreement about the chronology of this structural marker. Taboada, Bousquet & Philip (1993) established recurrence periods for two possible earthquakes of magnitude 6.7 Ms and 7.0 Ms, ranging from 1000 to 2000 yrs, respectively. These results were obtained assuming that the folding started at the end of the Pliocene (2

north.

The road from Benejúzar to stop 3.3 cuts across these conglomerates (approximately 1.3 km from Benejúzar). Also, it would be optionally possible to observe vertical dips in a quarry located 500 m eastward of the village of Hurchillo, on the road to Bigastro.

Transfer to Stop 3.3: After 1.4km you will come across a new sealed off road to the left (in a southerly direction). We can stop at this junction where there is some open ground with a few trees. On foot we will go south, climbing to the top of a limestone crest (a 5-minute walk) located to the left of the road.

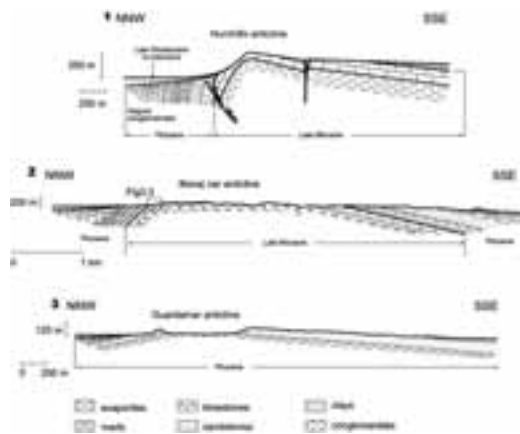


Figure 3.2 - Geological cross-sections of the asymmetric folds related to the Bajo Segura blind Fault. The Benejúzar anticline, located in the middle, is observable at stop 3.1. From Alfaro et al. (2002).

Ma) or at the beginning of Early Quaternary times (1.5 Ma). Bardají et al. (1995) deduced a Pleistocene age for this formation; which would mean a higher activity for this fault. Nonetheless, Alfaro et al. (2002), using micromammals, have dated the base of this Formation as Lower Pliocene (zone MN15). For this reason, Alfaro et al. (2002) suggest that the activity of the Bajo Segura Fault started earlier, approximately four million years ago.

Structural analysis of this marker indicates that deformation becomes more intense towards the west. Along the Hurchillo-Bigastro-Benejúzar road it can be seen how conglomerate strata dip steeply towards the north, or even vertically in the Hurchillo anticline. To the east, in the Benejúzar antiform, these strata dip approximately 50-60° to the north. And, close to the mouth of the Segura, in the Guardamar anticline, the Segura Conglomerate Formation dips 20° to the

Stop 3.3:
Bajo Segura Fault

(1:25.000 Map Benejúzar, IGN Series)

At this stop we can observe a spectacular hectometric fold located in the forelimb of the larger Benejúzar anticlinal structure (Fig. 3.2). Just two kilometres north of this area a high-resolution seismic profile indicates the existence of a monoclinical flexure. Finally, two kilometres to the east, the Lomas de la Juliana anticline has developed. Therefore, the northern limb of the Benejúzar anticline has a complex geometry, probably because the main Bajo Segura fault plane has several secondary splay faults close to the surface (Fig. 3.3).

In addition, from this stop there is a good panoramic view of the Bajo Segura Basin. The flat topography of the area is due to the last unit filling the Basin during the Late Pleistocene and the Holocene. These recent sediments are more than 30 m thick and have not had enough time to be appreciably deformed. The rapid sedimentation of these materials (varying between 3.7 mm/y and 1.9 mm/y) linked to the last eustatic sea-level rise obscures some geomorphological traces of the recent activity of this fault. These sediments constitute a multilayered aquifer with sediments highly susceptible to liquefaction. In the Bajo Segura Basin, indirect evidence of paleoearthquakes, such as seismic liquefaction, are of particular interest because surface fault ruptures are not visible. In this area, liquefaction occurred widely (over 7 km²) during the Torrevieja earthquake of 1829 as reported from many descriptive historical documents. The most frequent surface manifestations of seismic liquefaction during this historical earthquake were sand volcanos (with craters of up to 12 cm in diameter), lateral spreading



Figure 3.3 - Panoramic view of the hectometric fold observed at stop 3.3, on the forelimb of the Benejúzar anticline.

and numerous breaks and collapses, including the collapse of four bridges over the Segura river.

The search for paleoliquefaction features in the last sediments that fill the Bajo Segura Basin was unfruitful for two main reasons: (1) the water table is very shallow, and only 1 to 2 m of sediments are exposed above it, and (2) the uppermost layer, about 1 m thick, has been reworked by agricultural activity. In the study area, the only information available about recent paleoearthquakes comes from several seismite layers identified in core samples dating from the Late Pleistocene-Holocene (Alfaro et al., 1996). From the analysis of these seismite layers (25) and the radiometric C^{14} datings (17) corresponding to six boreholes, it is possible to identify seven paleoearthquakes over the last 8000 years. From these paleoearthquakes and the 1829 Torrevieja earthquake, we have established a minimum recurrence interval of earthquakes of moderate-high magnitude in the area of approximately 1000 years (Fig. 3.4).

Transfer to Stop 3.4: Return to Benejúzar. Take the CV-91 towards Almoradí-Guardamar. You will come to the A-37 where you need to turn north in the direction of Elche-Alicante. After going past the village of Catral, follow the signs to Murcia (A-7/E-15). Take the A-7/E-15 towards Murcia. Take the exit to Albaterra and continue until you come to the CV-873 (A-421). Take this road towards Hondón de los Frailes. Between kilometre 7.5 and 9.5 a spectacular progressive discordance in deposits of late Miocene and Pliocene can be seen, especially to the right. At the top of the slope we go past kilometre 11 and within less than 50 metres we come across a very sharp curve (be careful!). Right on this curve there is a dirt road leading off to the right. Go along this road for 50 metres until you come across the fault plane.

Stop 3.4:

Crevillente Fault

(1:25.000 Map Hondón de los Frailes, IGN Series)

The Crevillente Fault is an outstanding structure located in the eastern sector of the Betic Cordillera

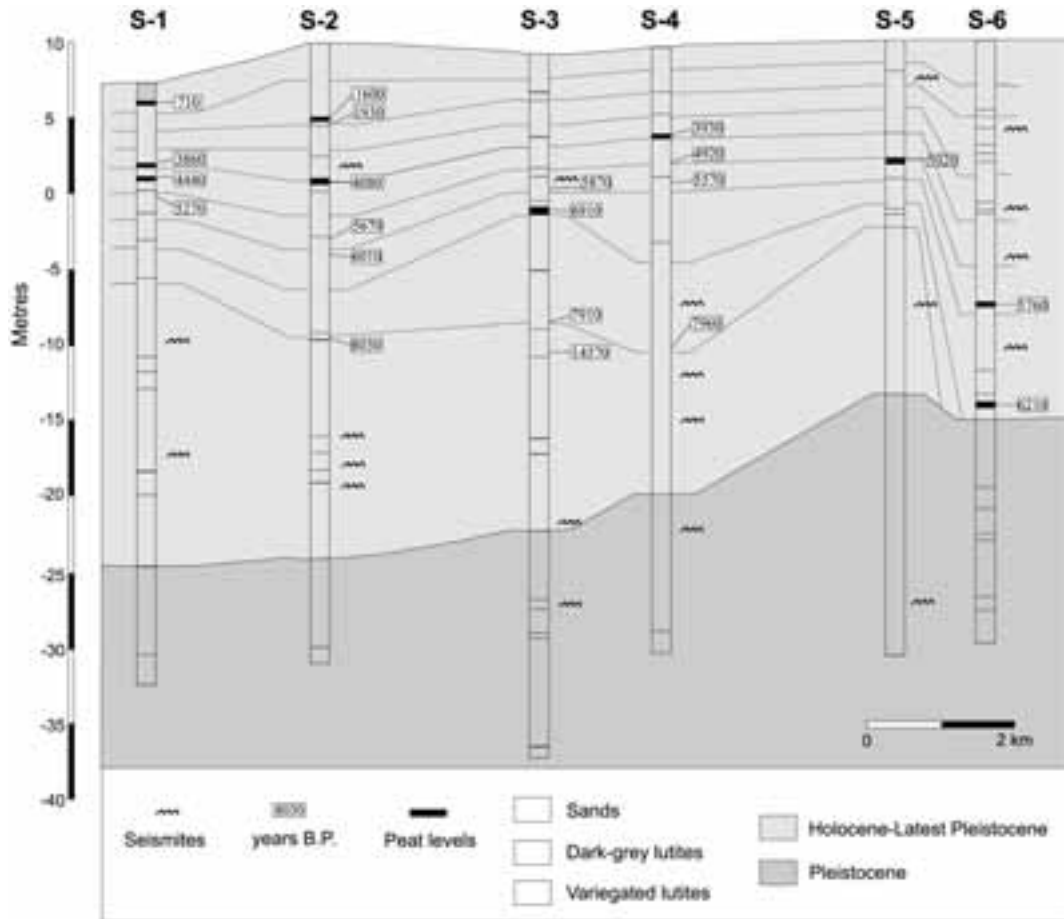


Figure 3.4 - Simplified geological cross-section of the uppermost unit of the Bajo Segura basin (Upper Pleistocene-Holocene), with the locations of boreholes, seismites and the C¹⁴ datings (from Alfaro et al., 2001).

(SE Spain). Its trace follows the contact between the External and the Internal Zones of the Betic Cordillera, the northern onshore Terminal Splay of the EBSZ, and the easternmost segment of the Cádiz-Alicante Fault zone. From the Late Miocene to the Quaternary, the kinematics of the Crevillente Fault remains unclear, probably due to its complex geological setting, and also because this fault has no clear superficial expression.

The ENE-WSW Crevillente Fault is a northwards dipping fault which deforms Mesozoic and Paleogene basement materials of the Betic External Zones, marine materials of the Early-Middle Miocene, as well as a sedimentary cover Late Miocene-Quaternary

in age (Fig.3.5). The fault can be divided into two main segments. One of them follows the southern edge of the Sierras of Abanilla and Crevillente. It comprises a several-hundred-metres-wide fault zone separating the Mesozoic basement materials of the External Zones from the Upper Miocene-Quaternary rocks. Along this segment, the geometry of the Upper Miocene-Quaternary strata is a progressive unconformity with internal angular unconformities. The older deposits, Tortonian in age, dip approximately 90°. The dip diminishes progressively, so that, the youngest Quaternary sediments become subhorizontal. Minor reverse and strike-slip faults occur along this segment, such as the small Albaterra NW thrust, where Lower Miocene rocks of Monte Alto thrusts Upper Miocene rocks.

Along the north-eastern Crevillente-Alicante segment, a set of Upper Miocene-Quaternary growth folds trending from N70E to N130E crop out (Elche,

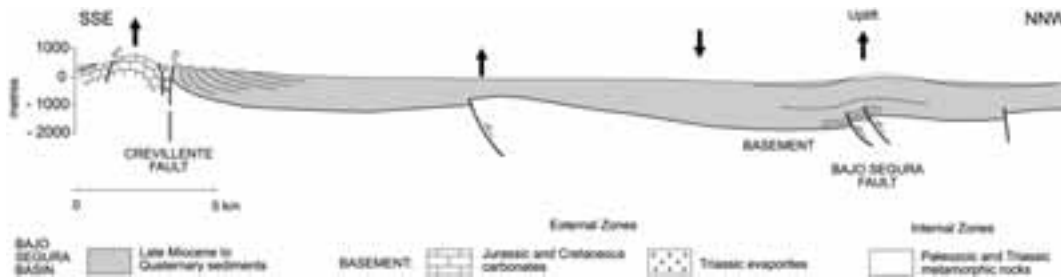


Figure 3.5 - Simplified geological cross-section of the Bajo Segura basin. The Crevillente Fault limits the northern part of the basin.

Sierra Gorda, Sierra Borbuño, San Juan), showing limbs formed by Upper Miocene-Quaternary syntectonic strata. The most deformed materials, Tortonian in age, dip less than those of the same age in the other segment. This different dip distribution is probably due to the fact that, in the western sector of the fault, the shortening is mainly concentrated in a unique deformational structure, which is related to the Crevillente Fault. In contrast, in the eastern part of the study area, the shortening is distributed through several folds along the Crevillente Fault, as well as others at La Marina and Santa Pola, situated further to the south.

Vertical movements occurred in the study area from the Late Miocene till the Present, which are related to the NW-SE shortening. The uplifted areas

correspond to growth anticlines, whilst the subsident areas are related to growth synclines. The largest uplift corresponds to the Sierra of Crevillente, where mountain chains close to 1000 m high are found (Fig. 3.5). This fault is also responsible for the subsidence of the southernmost sectors, where the Bajo Segura Basin is located. Geophysical studies (gravity, seismic profiles, and deep vertical electrical soundings) place the Triassic basement at more than 1000 m depth in Elche, near the Crevillente Fault (Gauyau et al., 1977). The resulting vertical uplift in this area, partially due to the activity of this fault has been more than 1000 m from Late Tortonian till the present day.

Along the Crevillente Fault there is much geological evidence of its recent activity. Certain Tyrrhenian coastal sediments east of Alicante are folded



Figure 3.6. - Detail of a fault plane in the Crevillente Fault zone which has deformed Quaternary deposits (note the oblique striae).

according to a N110-120E anticline (Bousquet and Philip, 1976). High-resolution seismic profiles across the eastern extension of the fault into the Mediterranean Sea also show the existence of compressive deformations in Quaternary sediments. In addition, at this stop Quaternary colluvial deposits deformed by this fault can be observed (Fig. 3.6). The Crevillente Fault has an associated seismicity characterized by low magnitude earthquakes (<5.0 mb). Only a focal mechanism has been calculated along its trace, and this corresponds to the 1981 earthquake ($m_b=4.9$). This earthquake, located in the marine prolongation of

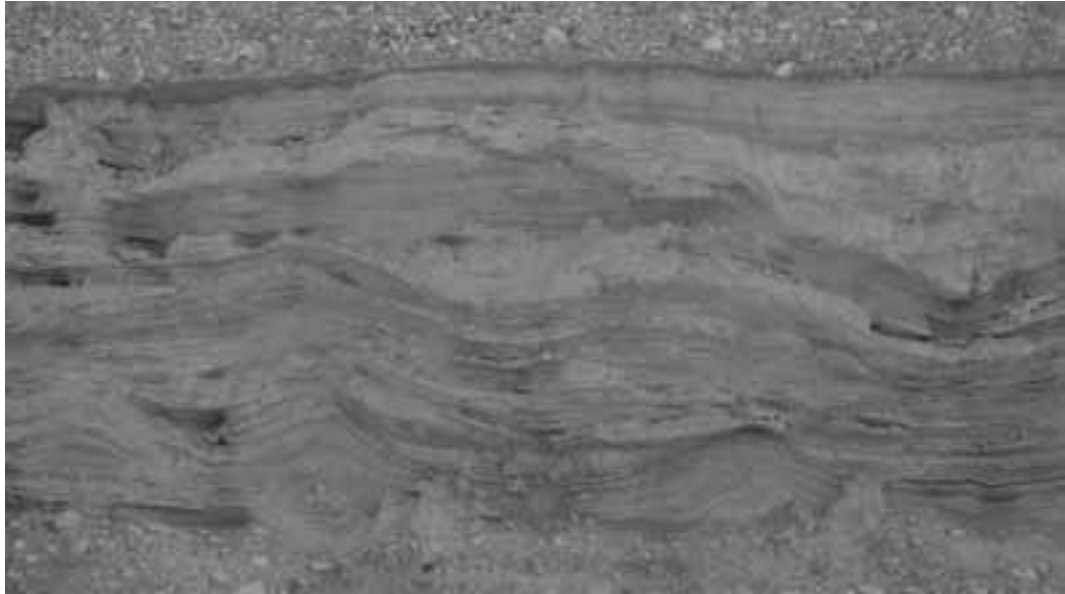


Figure 3.7 - Detail of the load structures interpreted as seismites in the Plio-Quaternary deposits of the Sierra del Colmenar.

the Crevillente Fault, has a reverse fault solution for its focal mechanism (Buforn and Udías, 1990). The ENE-WSW principal plane is consistent with the geological observations at the surface, as well as with the seismic profiles carried out in the continental shelf of Alicante.

Transfer to Stop 3.5: Go back along the CV-873 towards Albaterra and then take the A-7-E-15 towards Alicante. The last stop is located in the Sierra del Colmenar, at kilometre 701.4 of the A-7/E-15 motorway in the direction of Alicante (in a small rest area).

Stop 3.5:

Seismites (Sierra del Colmenar)

(1:25.000 Map Hondón de los Frailes, IGN Series)

At this stop several soft-sediment deformation structures interpreted as seismites can be observed. These seismites occur in deposits dated as Plio-Quaternary (Sucina Formation) by Montenat (1977), yet more recently considered as Lower to Middle Pleistocene (Goy et al., 1990).

The Sucina Formation is characterized by detrital layers with paleosoils formed in a continental environment. Lobes, 50 cm wide and one metre thick on average, show downward convexity (sagging load casts) and are limited above and below by non-deformed beds (Fig. 3.7).

DAY 4

The Catalan Coastal Ranges: El Camp Fault.

E. Masana and P. Santanach.

This part of the field trip shows one example of the normal faults that constitute the emerged sector of the Valencia Trough in the Catalan Coastal Ranges: the El Camp fault. This fault bounds the El Camp Neogene basin which is infilled by 2000 m of Miocene sediments and Quaternary alluvial fans next to the fault. Some of these alluvial fans have been affected by the most recent movements of the El Camp fault and show a number of fault scarps. The most prominent of these is the 25-30 km long Montroig fault scarp where a complete paleoseismological analysis was performed by trenching (Masana et al, 2001 a, b, Santanach et al., 2001).

Transfer to Stop 4.1: Leaving Cambrils by road T-312 (going inland) we'll arrive at Montbrió del Camp, where we'll turn to the southeast following road T-310 towards Montroig del Camp. After reaching this village and take the T-322 road to Colldejou. About three km after having taken this new road, turn right and head up to the La Roca sanctuary. Leave the car in the parking area and walk to the sanctuary balcony.

Stop 4.1:

Mare de Déu de la Roca (Montroig del Camp). Setting and Introduction.

(1:50.000 Map Baix Camp, ICC Series).

From this vantage point the southern part of the El Camp fault front and of the Quaternary basin

Transfer to Stop 4.2: Head back along the T-322 road the way we came, coming to Monroig. Cross this town taking T-310 towards Reus. Approximately 1 km northeast from the village we will stop at a fruit store where parking is available.

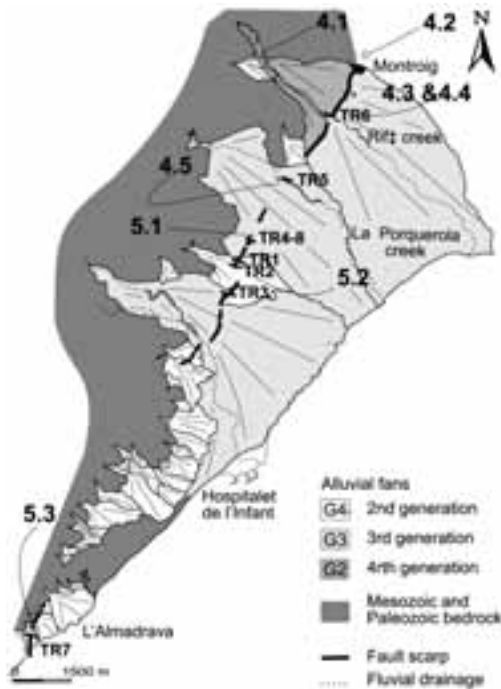


Figure 4.1 - Geomorphological map of the southern part of the Monroig fault scarp showing the most important generations of alluvial fans outcropping in the area. Numbers indicate the excursion stops.

infilling can be observed. An introduction to the regional setting and to the El Camp geology will be done at this stop, starting off from this panoramic view. The normal faulting along the El Camp fault can be directly observed. Also, the different alluvial fan generations can be distinguished, with the Rifà alluvial fan being the best defined from here.

The El Camp fault, with a cumulative slip-rate since the Aquitanian (or the Burdigalian) of 0.12 (0.16) mm/yr, is the last normal fault to the northwest in the Iberian margin. Therefore, its total vertical slip-rate is higher than the rest of the faults owing to the shoulder effect, which normally takes place only in the limits of extensional systems.

Stop 4.2:

Monroig fault scarp.

(1:50.000 Map Baix Camp, ICC Series)

The Monroig fault scarp (Fig. 4.1) is a more than 25 km long, NNE-SSW trending scarp which affects different generations of Quaternary alluvial fans in the El Camp southern fault. Up to four generations of alluvial fans have been described according to

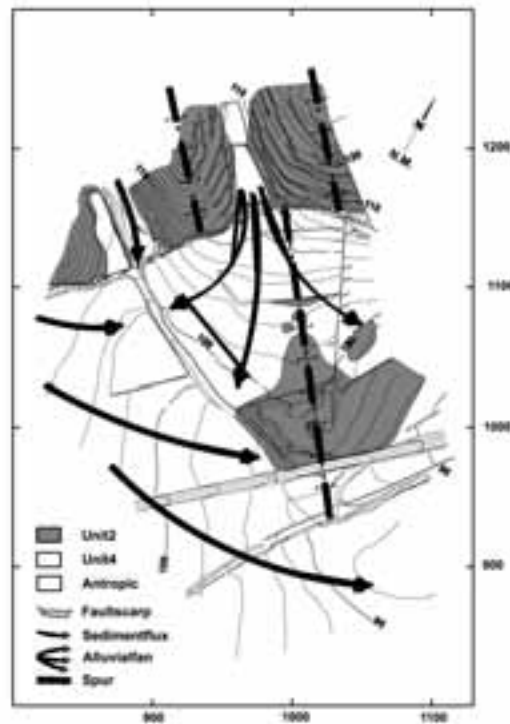


Figure 4.2 - Microtopographical map of the trench 0 area across the Monroig fault scarp, north of Rifà creek. Unit 2 (G2) outcropping in the downthrown wall shows an elongated spur that should have its continuation in the upthrown block. Two spurs are present in the latter one, though the fact that none of them is aligned with the former suggests a strike slip. Therefore, the uncertainty lies on which of the two crests in the footwall correlates with the crest in the footwall. This is the only evidence of a strike component found along the fault.

their geomorphological signature and stratigraphic elements. Three of them are of interest for the Montroig scarp analysis: G2, G3, and G4, (from oldest to youngest). The interaction between these units and the fault itself gave rise to a segment boundary at La Porquerola creek: to the north G3 and G4 have not been affected by the fault activity, whereas to the south they clearly have. The age of these alluvial fans has been established first by correlation with the last isotopic O stages, and also by U/Th and Thermoluminescence dating of the calcrete soils developed on their top. Paleomagnetism was also used to narrow the age. Dating results reveal that G3 is probably older than 125 ka, and G2 older than 300 ka (age of the soils). The northern segment ceased its activity before the end of sedimentation of G3, i.e. before 125 ka, whereas, the southern segment remained active after G4, i.e. it is younger than 125ka.

Transfer to Stop 4.3: Go back to road T-310 and cross through Montroig heading south. At about 1 km south of the crossroad to Colldejou park the car.

Stop 4.3:

Trench 0 site.

(1:50.000 Map Baix Camp, ICC Series)

In this stop we can visit part of the fault scarp and the site of trench 0. This trench was dug in a small gully that eroded the fault scarp and deposited sediments over it. As a consequence of the high sedimentation rate compared to the low uplift rate, trench 0 did not reach the faulted sediments.

The detailed microtopography of this site (Fig. 4.2) also allows for the quantification of the fault's strike-slip. This is done by correlating a buried crest in the downthrown wall with one of the two crests in the upthrown wall, giving us 40-60 m of horizontal offset while, in this site, the vertical offset is 17 m (maximum). This is the only site where this horizontal component was observed along the scarp.

Transfer to Stop 4.4: Take T-310 again for less than

500 m, and cross the main channel of the Rifà alluvial fan on a bridge. Twenty meters after the bridge turn right and take an unpaved road running parallel to the channel. Park after 100 m.

Stop 4.4:

Barranc de Rifà.

(1:50.000 Map Baix Camp, ICC Series)

The Rifà alluvial fan corresponds to the G3 generation of fans and its main channel crosses the Montroig fault scarp perpendicularly. This stop allows the observation of the Montroig fault outcropping at the deepest part of the main channel. This fault, according to the results of trench 6 dug at this site, has been sealed here by the sediments belonging to the upper part of generation G3. At the surface, G3 forms a fluvial terrace which also seals the morphological fault scarp; consequently no morphological fault scarp is observed here.

Transfer to Stop 4.5: Following road T-310 to the south, we will stop on the next alluvial fan, 2m away from stop 4.4. We will follow the main channel of the Porquerola alluvial fan to the southeast for 200 m.

Stop 4.5:

La Porquerola creek.

(1:50.000 Map Baix Camp, ICC Series)

On this stop we will visit the site of trench 5, which was dug on the northeastern side of the channel. This site clearly shows the Montroig fault, as well as a good exposure of the gentle flexure it generates in the G2 and G3 alluvial fans (Fig. 4.3). As a consequence of this flexure, some extensional fractures are outcropping on the folded G2 layers, which also present evidence of liquefaction, clearly linked to the seismogenic nature of the fault. These structures are only present near the fault and following open cracks trending NNE-SSW (i.e. parallel to the Montroig fault).

Trench 5 (Fig. 4.3) shows G3 affected by the Montroig fault and, therefore, relates the morphological scarp detected at the surface with fault activity after 125 ka.

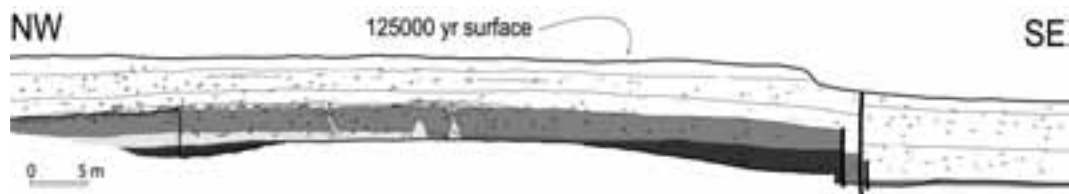


Figure 4.3. Cross-section of the La Porquerola creek. Note the Montroig fault across the sediments and the small fault scarp at surface. The upper portion of this cross-section was constructed in part using the data obtained in trench 5.

This suggests that the Porquerola creek itself belongs to the southern segment (the active one), while to the north of it (the previous stop), G3 has not been affected by the fault. The segment boundary is located, thus, between the Rifà and Porquerola fan channels.

south until you cross a small bridge, 1 km south from stop 4.5. Turn left and take an unpaved road for 300 m.

DAY 5

**The Catalan Coastal Ranges:
El Camp Fault.**

E. Masana and P. Santanach.

Transfer to Stop 5.1: Take the same T-310 road to the

Stop 5.1:

Trenches 4 and 8 sites. Visit to open trench 4.

(1:50.000 Map Baix Camp, IGN Series)

This stop will be devoted to making observations in an open trench (trench 4) and the site of trench 8 (buried) (Fig. 5.1). The site clearly shows the location of the Montroig fault scarp which offsets the surface of the G3 alluvial fan. Trench 4 exposed the Montroig

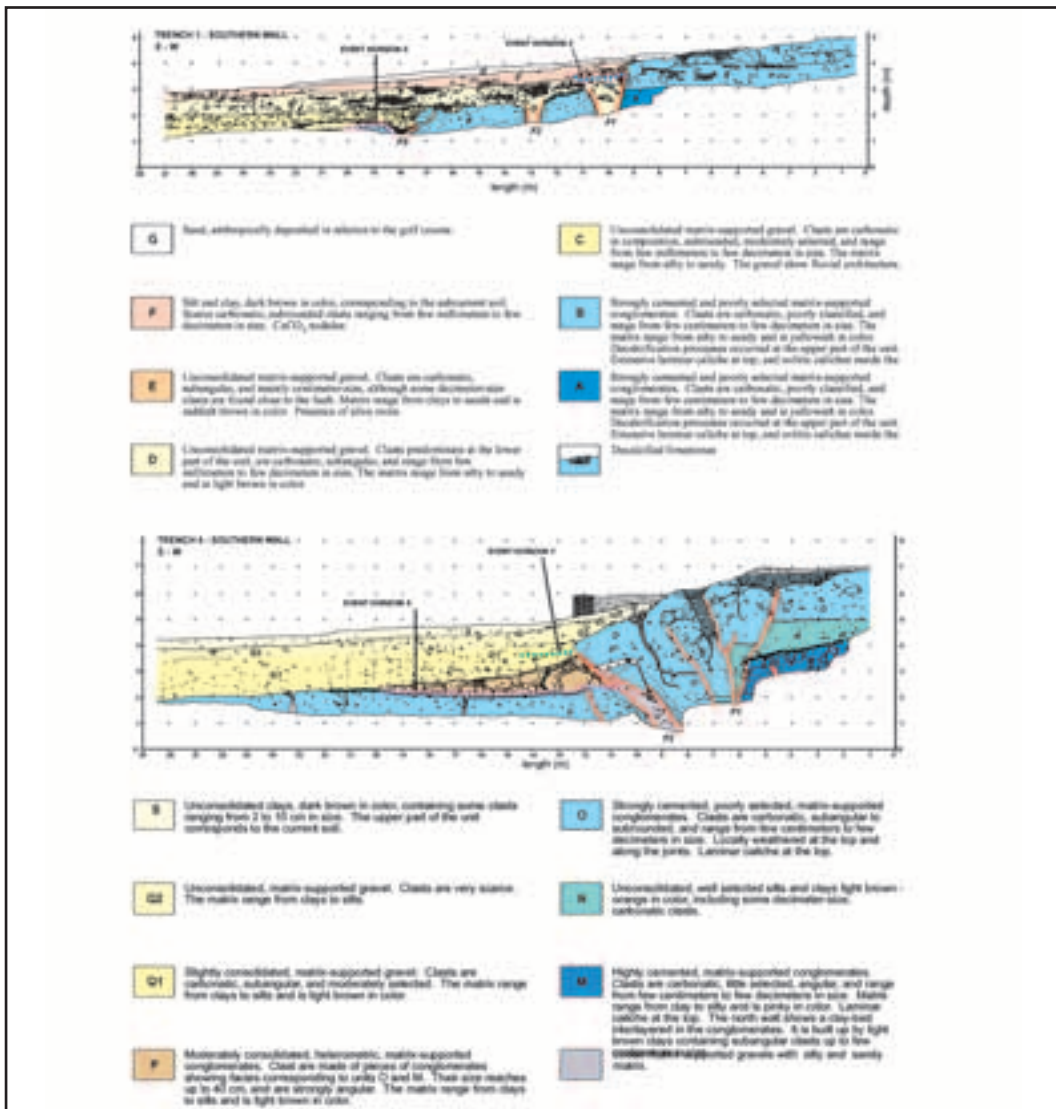


Figure 5.1. Logs of trenches 1 and 4. Modified from Masana et al., (2001a).

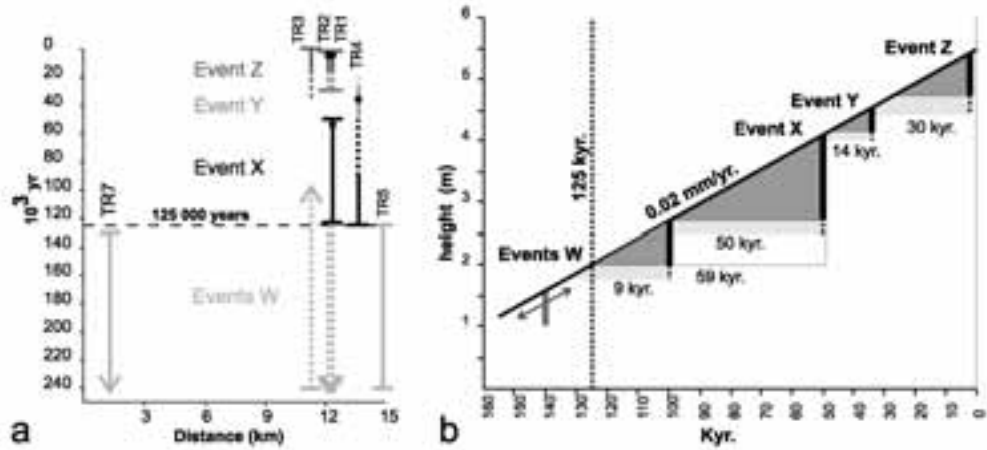


Figure 5.2 - Sketch of the events detected in the paleoseismological analysis and their age constraint. Events W was not described in the text as it has not been clearly dated. A black dot indicates the most creditable time position for each event. b) Cumulative height versus time plot of the El Camp fault estimated from the paleoseismic results obtained. Estimated inter-seismic periods are also indicated. Modified from Masana et al., (2001a).

fault and revealed the relationship between sediments and faulting, which was used to establish two seismic events along this fault. The most recent event was dated by U/Th, Thermoluminescence, and pollen analysis in the Holocene, while the previous event, which displays an evident fault colluvial wedge, has been dated to between 125 and 50 ka.

Transfer to Stop 5.2: We will go back to road T-310 and follow it to the south for less than 1 km, until we reach a cross road to the left, which we will take for 500 m. We will then enter the Bonmont Terres Noves golf club, to the right, after having crossed the fault scarp reflected in the road's profile.

Stop 5.2:

Trenches 1 and 2 site.

(1:50.000 Map Reus, ICC Series)

The Montroig fault affects G4 alluvial fans (the youngest) only in two locations: in the golf club and, further south, in an area that has been completely modified. The golf club is, therefore, the only place for studying the most recent movements of the fault, and was selected as the site for digging trenches 1 and 2, currently buried (Fig. 5.1). The surface of the G4 alluvial fan is here offset three meters, while the surface of G3, located several tens of meters to the north, is offset ten meters. These trenches showed the Montroig fault and revealed evidence of two large earthquakes. The most recently detected event, with

1 m offset, was dated as younger than 3000 yrs and the oldest, post-125 ka, was correlated with the oldest event detected in trench 4. This stop will be devoted to visiting the site of these trenches and to discussing the results obtained.

Transfer to Stop 5.3: Return to road T-310 and follow it to the south until it branches in two. Take T-318 which will bring us to C-233. We will then use this road to reach the National 340 road in Hospitalet de l'Infant. There we will go to the south for 6 km where we can see the Vandellós Nuclear Power Plant to the left, between the road and the seaside. Take the Almadrava road to the left and reach Almadrava beach, where we will park. There we will walk to the north, parallel to the coast, towards the nuclear power plant installation.

Stop 5.3:

Almadrava Nuclear Power Plant site.

Visit to an old trench site.

(1:50.000 Map Baix Camp, ICC Series)

On this stop we will visit the southernmost expression of the Montroig fault scarp. The fault enters the sea and therefore probably is longer than what is observed in the emerged sector, although no data is available concerning this offshore part. Several outcrops can be visited at this site to observe different aspects of the Montroig fault. Some of them are natural and show liquefaction structures along the fractures, flexure of

the upper layers, and also normal fault scarps at the surface. Some others are artificial and were dug at the time of the nuclear power plant's construction to bracket the activity of the fault. This includes a trench which was dug mostly in the uplifted part of the fault. This trench was re-analyzed during the DATACIÓN project (Santanach et al., 2001) and some U/Th and TL dating were performed on it. Evidence of past events was detected along it.

A synthesis of the paleoseismological results will be made at this stop (Fig 5.2). The recent tectonic activity of this fault is demonstrated by a young mountain front and a fault scarp cutting Quaternary alluvial fans. The regional geological analysis indicates that three generations of alluvial fans are cut by the fault. Absolute (TL and U/Th) and relative dating both show that the oldest fan is 300 ka old and the intermediate one is 125 ka old. The study of 8 trenches and absolute dating, TL, U/Th, radiocarbon, as well as pollen analysis revealed the following: 1) The El Camp fault consists of two segments limited at the Porquerola creek, and that only the southern segment has been active since 125 ka. 2) The fault is seismogenic because it is directly associated with liquefaction features and with colluvial wedges. 3) The El Camp fault has produced a minimum of three well-constrained surface-rupturing earthquakes since 125 ka (events X, Y, and Z). On the basis of the different tectonic features observed in the trenches, the recurrence period of large earthquakes during this timeperiod is estimated to be around 30 ka, and the elapsed time since the most recent event, to be around 3000 yrs. Using the fault length and the vertical displacement per event, the largest estimated earthquake had a magnitude of Mw 6.7. These results considerably improve our understanding of the seismic hazard of the region and illustrate how paleoseismology can contribute to the seismic hazard assessment in areas of low or no historical seismicity, as is the case in most of the Iberian Peninsula.

Acknowledgments

This work has been carried out within the framework of the following research projects: BTE2002-1691(USAL), BTE2002-1065 (CSIC), BTE2000-0299 (UA) and AMB97-0523(UCM) funded by the Spanish DGES; the Datación project (UB) co-funded by the Consejo de Seguridad Nuclear (CSN) and the Empresa Nacional de Residuos Radioactivos S.A (ENRESA) with the contribution of the Vandellós II Nuclear Power Plant; project CTIBID/2002/177

funded by the Generalitat Valenciana; and the SAFE project (ENV-2000-22005) funded by the European Union. This work is dedicated to the memory of Professor J.L. Hernández-Enrile(UCM, Spain) who passed away in April 2003. He devoted most of his research to the study of the neotectonics of the Eastern Betic Cordillera, and contributed invaluable to the geologic understanding of the area visited on this field trip.

References cited

- Alfaro, P., Delgado, J., Estévez, A. and López-Casado, C. (2001). Paleoliquefaction in the Bajo Segura basin (eastern Betic Cordillera) *Acta Geol. Hisp.*, 36 (3-4), 233-244.
- Alfaro, P., Andreu, J.M., Delgado, J., Estévez, A. Soria, J.M. and Teixidó, T. (2002a). Quaternary deformation of the Bajo Segura blind fault (eastern Betic Cordillera) revealed by high-resolution reflection profiling. *Geological Magazine*, 139, 3, 331-341.
- Alfaro, P., Delgado, J., Estévez, A. Soria, J.M. and Yébenes, A. (2002b). Onshore and offshore compressional tectonics in the eastern Betic Cordillera (SE Spain). *Marine Geology*, 186, 337-349.
- Armijo, R. (1977). La zona des failles Lorca-Totana (Cordillères Bétiques, Espagne). Etude tectonique et neotectonique. Thèse 3^e cycle. Paris VII. 229 pp.
- Banda, E. and Santanach, P. (1992): The Valencia Trough (western Mediterranean): an overview: *Tectonophysics*, 208, 183-202.
- Banks, C.J. and Warburton, J. (1991). Mid-Crustal detachment in the Betic and Pyrenean systems of eastern Spain. *Tectonophysics*, 191, 275-289.
- Bardají, T., Goy, J.L., Mörner, N.A., Zazo, C., Silva, P.G., Somoza, L., Dabrio, C., Baena, J. (1995). Towards a Plio-Pleistocene chronostratigraphy in Eastern Betic Basins (SE Spain). *Geodinamica Acta*, 8, 112-126.
- Bell, J.W., Amelung, F. and King, G.C.P. (1997). Preliminary late Quaternary history of the Carboneras Fault, Southeastern Spain. *J. Geodynamics*, 24, 51-66.
- Bousquet, J. C. (1979). Quaternary strike-slip faults in southern Spain. *Tectonophysics*, 52, 277-286
- Bufforn, E., Udias, A. and Mezcua, J. (1990). Seismicity and focal mechanisms in south Spain. *Bull. Seismol. Soc. Am.*, 78, 2008-2024.
- Bousquet, J.C. (1979). Quaternary strike-slip faults in southeastern Spain. *Tectonophysics*, 52. 277-286.
- Bousquet, J.C. and Montenat, C. (1974). Presence décrochements NE-SW plio-quaternaires dans

- les Cordillères Bétiques (Espagne). Extension et signification général. *C. R. Acad. Sci. Paris*, 278, 2617 – 2620.
- Bousquet, J.C. and Phillip, H. (1976). Observations microtectoniques sur la compression nord-sud quaternaire des Cordillères bétiques orientales (Espagne meridionale – Arc de Gibraltar). *Bull. Soc. Geol. France*, 28 (3), 711-724
- Clothing, S., Burov, E., Beekman, F., Amdeweg, B., Andriessen, P.A., García-Castellanos, D., de Vicente, G. and Vegas, R. (2002). Lithospheric folding in Iberia. *Tectonics*, 21 (5), 1041, doi: 10.1029/2001TC901031.
- Coppier, G., Ott D'Estevou, P., and Montenat, C. (1990). Kinematics and paleogeographical evolution of the eastern Almería basins. *Doc. et Trav. IGAL*, 12/13, 189-193.
- Faulkner, D.R., Lewis, A.C. and Rutter, E.H. (2003). On the internal structure and mechanics of large strike-slip fault zones: field observations of the Carboneras fault in Southeastern Spain. *Tectonophysics*, 367, 235-251.
- Fontboté, J. M. (1954): Las relaciones tectónicas de la depresión del Vallès-Pendès con la Cordillera Prelitoral y con la depresión del Ebro, in Tomo Homenaje al profesor E. Hernandez Pacheco, *R. Soc. Esp. Hist. Nat.*, 281-310.
- Fontboté, J.M., Guimera, J., Roca, E., Sabat, F., Santanach, P. and Fernández-Ortigosa, F. (1990). The geodynamic evolution of the Valencia trough (Western Mediterranean). *Rev. Soc. Geol. Esp.*, 3, 249-259.
- Galindo Zaldívar, J., Jabaloy, A., Serrano, I., Morales, J. and González-Lodeiro (1999). Recent and present-day stresses in the Granada basin (Betic Cordillera: Example of a late Miocene-present day extensional basin in a convergent plate boundary. *Tectonics*, 18, 686-702.
- Gauyau, F., Bayer, R., Bousquet, J.C., Lachaud, J., Lesquer, A. and Montenat, C. (1977). Le prolongement de l'accident d'Alhama de Murcia entre Murcia et Alicante (Espagne Meridionale): Résultats d'une étude géophysique. *Bull. Soc. Geol. France*, 7 (19), 623-632.
- Gómez, M. and Guimerà, J. (1999): Estructura alpina de la Serra de Miramar y del NE de les Muntanyes de Prades (Cadena Costera Catalana). *Rev. Soc. Geol. España*, 12 (3-4), 405-418.
- Goy, J.L. and Zazo, C. (1984). Los piedemontes cuaternarios de Campo Dalías y Campo de Nijar (Almería). *Cuad. Lab. Xeol. Laxe*, 5, 40-53.
- Goy, J.L. and Zazo, C. (1986). Synthesis of the Quaternary in the Almería littoral, neotectonic activity and its morphologic features, Eastern Betics, Spain. *Tectonophysics*, 130, 259-270.
- Goy, J.L. and Zazo, C. (1989). The role of neotectonics in the morphologic distribution of the Quaternary marine and continental deposits of the Elche Basin, Southeast Spain. *Pal., Pal., Pal.*, 68, 219-225.
- Goy, J.L., Zazo, C., Somoza, L., Dabrio, C.J. (1990). Evolución paleogeográfica de la Depresión de Elche-Cuenca del Bajo Segura (España) durante el Pleistoceno. *Estudios Geol.*, 46, 237-244.
- Hernández Enrile, J.L., Martínez-Díaz, J.J., Masana, E. and Santanach, P. (2000). Resultados preliminares del estudio paleosísmico mediante trincheras de la Falla de Alhama de Murcia (Cordillera Bética). *Geotemas*, 1(4), 335-339.
- Herraiz, M., de Vicente, G. et al. (2000). The recent (upper Miocene to Quaternary) and present tectonic stress distributions in the Iberian Peninsula. *Tectonics*, 19, 762-786.
- Hillaire Marcel, C., Carro, O., Causse, C., Goy, J.L. and Zazo, C. (1986). Th/U dating on *Strimbus* *hubonius* bearing marine terraces in southern Spain. *Geology*, 14, 613-616.
- Keller, J.V.A., Hall, H., Dart, C.J., and McClay, K.R. (1995). The geometry and evolution of transpressional strike-slip system: the Carboneras fault, SE Spain, *J. Geol. Soc. London*, 152, 339-351.
- Larouzière, D., Bolze, J., Bordet, P., Hernández, J., Montenat, C. and Ott D'Estevou, P. (1988) The Betic segment of the lithospheric Transalboran Shear Zone during the Late Miocene. *Tectonophysics*, 152, 41-52.
- Lonergan, L. (1993). Timing and kinematics of deformation in the Maláguide Complex, Internal Zone of the Betic Cordillera. *Tectonics*, 12, 460-467.
- Martí, J., Mitjavila, J., Roca, E., and Aparicio, A., (1992): Cenozoic magmatism of the Valencia trough (western mediterranean): relationship between structural evolution and volcanism. *Tectonophysics*, 103, 145-166.
- Martínez-Díaz, J.J. (1999). Sismotectónica de la Falla de Alhama de Murcia: Implicaciones sismogénicas del Terremoto de Lorca de Junio-1977 (Mb: 4,2). *Estudios Geol.*, 55, 251-266.
- Martínez-Díaz, J.J. and Hernández Enrile, J.L. (2001). Using travertine deformations to characterize paleoseismic activity along an active oblique-slip fault: the Alhama de Murcia fault (Betic Cordillera, Spain). *Acta Geol. Hisp.*, 36 (3-4), 297-314.
- Martínez-Díaz, J.J., Hernández Enrile, J.L., Alfaro, P. and Estévez, A. (2000). Neotectónica y Tectónica

- activa en la Cordillera Bética Oriental (sectores de Lorca-Totana y Bajo Segura). In: "Itinerarios Geológico por la Provincia de Alicante y limítrofes" (J.C. Cañavereas et al. Eds.), pp.75-88. V Congreso Español de Geología (guidebook), Universidad de Alicante, Alicante (Spain).
- Martínez-Díaz, J.J., Masana, E., Hernández Enrile, J.L. and Santanach, P. (2001). Evidence of coseismic events of recurrent prehistoric deformation along the Alhama de Murcia fault (SE Spain). *Acta Geol. Hisp.*, 36 (3-4), 315-328.
- Martínez-Díaz J.J. and Hernández-Enrile, J.L. (in press). Neotectonics and morphotectonics of the southern Almería region (Betic Cordillera-Spain). Kinematic implications. *International Journal of Earth Sciences*, in press.
- Masana, E. (1994). Neotectonic features of the Catalan Coastal Ranges, Northeastern Spain. *Acta Geol. Hisp.*, 29 (2-4), 107-121.
- Masana, E. (1996). Evidence for past earthquakes in an area of low historical seismicity: the Catalan coastal ranges, NE Spain. *Annali di Geofisica*, 39(3), 689-704.
- Masana, E., Villamarín, J.A., Sánchez Cabañero, J., Plaza and Santanach, P. (2001a): Seismogenic faulting in an area of low seismic activity: Paleoseismicity of the El Camp fault (Northeast Spain). *Geol. Mijnbouw/Netherlands J. Geosciences*, 80 (3-4), 29-41.
- Masana, E., Villamarín, J.A. and Santanach P. (2001b). Paleoseismic results from multiple trenching analysis along a silent fault: The El Camp Fault (Tarragona, NE Peninsula Ibérica. *Acta Geol. Hisp.*, 36 (3-4), 329-341.
- Masana, E. Martínez-Díaz, J.J., Hernández Enrile, J.L., and Santanach, P. (2004). Constraining seismotectonics in a diffuse collisional plate boundary by paleoseismic results. A preliminary approach along the Alhama de Murcia Fault (Betic Cordillera). *J. Geophys. Res.*, 109, B01301, doi: 10.1029/2002JB002359, 2004
- Mather, A.E., Martín, J.M., Harvey, A.M. and Braga, J.C. (2001). "A Field guide to the Neogene sedimentary basins of the Almería province, south-east Spain". Blackwell Science Ltd., Oxford, USA. 350 pages.
- Mezcua, J., Herraiz, M. and Buffon, E. (1984). Study of the 6th June 1977 Lorca (Spain) Earthquake and its aftershock sequence. *Bull. Seismol. Soc. Am.*, 74. 167-179
- Montenat, C., (1977). "Les bassins néogènes et quaternaires du Levant d'Alicante à Murcie (Cordillères Bétiques orientales, Espagne). *Stratigraphie, paléontologie et évolution dynamique*". Ph. D. Thesis Laboratoire de Géologie, University of Lyon, 69, 345 pages.
- Montenat, C., Ott d'Estevou, Ph. and Masse, P. (1987). Tecto-sedimentary characters of the Betic Neogene basins evolving in a crustal transcurrent shear zone (SE Spain). *Bull. Centre Rech. Explor. Proc. Elf-Aquitaine*, 11, 1-22.
- Platt, J.P. and Vissers, R.L. (1989). Extensional Collapse of thickened continental lithosphere. A working hypothesis for the Alboran Sea and Gibraltar Arc. *Geology*, 17, 540-543.
- Reicherter, K.R. and Reiss, S. (2001). The Carboneras Fault Zone (southeastern Spain) revisited with Ground Penetrating Radar – Quaternary structural styles from high resolution images. *Geol. Mijnbouw*, 80 (3-4), 129-138.
- Roca, E. (1996): La evolución geodinámica de la Cuenca Catalano-Baleares y áreas adyacentes desde el Mesozoico hasta la actualidad. *Acta Geol. Hisp.*, 29 (1994), 3-26.
- Roca, E. and Guimerà, J., (1992): The neogene structure of the eastern Iberian margin: structural constraints on the crustal evolution of the Valencia trough (Western Mediterranean). *Tectonophysics*, 203, 203-218.
- Rutter, E. H., Maddock, R.H., Hall, S.H. y White, S. (1986). Comparative microstructures of natural and experimentally produced clay-bearing fault gouges. *Pageoph.* 124. 1-2: 1-30.
- Sabat, F., Roca, E., Muñoz, J.A., Vergés, J., Sans, M., Masana, E., Santanach, P. Estévez, A. and Santisteban, C. (1995): Role of extension and compression in the evolution of the eastern margin of Iberia: the ESCI-València Trough seismic profile. *Rev. Soc. Geol. España*, 8 (4), 431-448.
- Santanach, P., Masana, E. and Villamarín, J.A. (2001): "Proyecto Datación. Madrid", Consejo de Seguridad Nuclear, 159 pages.
- Sanz de Galdeano, C. (1990). Geologic evolution of the Betic Cordillera in the western Mediterranean, Miocene to present. *Tectonophysics*, 172, 107-119.
- Sanz de Galdeano, C., López Casado, C., Delgado, J., and Peinado, M.A. (1995). Shallow seismicity and active faults in the Betic Cordillera: a preliminary approach to seismic sources associated with specific faults. *Tectonophysics*, 248, 293-302.
- Silva, P.G. (1996). Geometría fractal de la Zona de Falla de Lorca-Alhama (Murcia, SE España). *Geogaceta*, 20(6). 141-144.
- Silva, P.G., Harvey, A.M., Zazo, C. and Goy, J.L. (1992a). Geomorphology, depositional style and

- morphometric relationships of Quaternary alluvial fans in the Guadalentin Depression (Murcia, SE Spain). *Z. F. Geomorph.*, 36, 661-673.
- Silva, P.G., Goy, J.L. and Zazo, C. (1992b). Características estructurales y geométricas de la Zona de Falla de Lorca-Alhama, *Geogaceta*, 12, 7-11.
- Silva, P.G., Goy, J.L., Somoza, L., Zazo, C. and Bardají, T. (1993). Landscape response to strike-slip faulting linked to collisional settings: Quaternary tectonics and basin formation in the Eastern Betics, Southeast Spain. *Tectonophysics*, 224, 289-303.
- Silva, P.G., Goy, J.L., Zazo, C., Lario, J. and Bardají, T. (1997). Paleoseismic indications along "aseismic" fault segments in the Guadalentin Depression (SE Spain). *J. Geodynamics*, 24, 105-115.
- Silva, P.G., Goy, J.L., Zazo, C. and Bardají, T. (2003). Fault generated mountain fronts in southeast Spain: geomorphologic assessment of tectonic and seismic activity. *Geomorphology*, 203-226.
- Stich, D., Ammon, C.J. and Morales, J. (2003). Moment tensor solutions for small and moderate earthquakes in the Ibero-Maghreb region. *J. Geophys. Resch.*, 108 (B3), 2148, doi: 10.1029/2002JB002057.
- Taboada A., Bousquet J.C., Philip H., (1993). Coseismic elastic models of folds above blind thrusts in the Betic Cordilleras (Spain) and evaluation of seismic hazard. *Tectonophysics*, 220, 223-241.
- Vogt (1972): Les tremblements de terre en France. *Mém. B.R.G.M.*, 96, Orleáns, France.
- Weijermars, R., (1987). The Palomares brittle-ductile shear zone of southern Spain. *J. Struct. Geol.*, 9, 139-157.
- Weijermars, R. (1991). Geology and tectonics of the Betic Zone, SE Spain. *Earth Science Reviews*, 31, 153-236.
- Zazo, C., Goy, J.L., Bardají, T., Dabrio, C.J. and Somoza, L. (1989). "The Mediterranean Littoral". Exc. B1 2ª Reunión de Cuaternario Ibérico, AEQUA, Madrid, 127 pages.
- Zazo, C., Goy, J.L., Dabrio, C.J., Bardají, T., Somoza, L. and Silva, P.G. (1993). The Last Interglacial in the Mediterranean as a model for the present Interglacial. *Global and Planetary Change*, 7, 109-117.
- Zazo, C., Bardají, T., Dabrio, C.J., Goy, J.L., Hillaire-Marcel, Cl. (1998). "Record of late Pliocene and Quaternary Sea-Level Changes in Coastal settings, Southeast Spain". pp. 151-169 15th Int. Sedimentological Congress IAS (Alicante-1998), Field Trip Guide Book
- Zazo, C., Goy, Dabrio, C.J., Bardají, T., Hillaire-Marcel, Cl., Ghaleb, B., González-Delgado, J.A., Soler, V. (2003). Pleistocene raised marine terraces of the Spanish Mediterranean and Atlantic coast: record of coastal uplift, sea level highstands and climate changes. *Marine Geology*, 194, 103-133.

Back Cover:
field trip itinerary

FIELD TRIP MAP

32nd INTERNATIONAL GEOLOGICAL CONGRESS



Edited by APAT